Analysis of Reduced and Oxidized Nitrogen-Containing

Organic Compounds at a Coastal Site in Summer and Winter

Jenna C. Ditto[1,†], Jo Machesky[1], and Drew R. Gentner[1,*]

[1] Department of Chemical and Environmental Engineering, Yale University,

New Haven, CT, 06511, USA

[†] Now at: Department of Chemical Engineering and Applied Chemistry, University of Toronto,

Toronto, ON, M5S 3E5, Canada

* Correspondence to: drew.gentner@yale.edu

Abstract

Nitrogen-containing organic compounds, which may be directly emitted to the atmosphere or may form via reactions with prevalent reactive nitrogen species (e.g., NH_3, NO_x, NO_3), have important but uncertain effects on climate and human health. Using gas and liquid chromatography with soft ionization and high-resolution mass spectrometry, we performed a molecular-level speciation of functionalized organic compounds at a coastal site on the Long Island Sound in summer (during the LISTOS 2018 campaign) and winter. This region often experiences poor air quality due to the emissions of reactive anthropogenic, biogenic, and marine-derived compounds and their chemical transformation products. We observed a range of functionalized compounds containing oxygen, nitrogen, and/or sulfur atoms resulting from these direct emissions and chemical transformations, including photochemical and aqueous-phase processing that were more pronounced in summer and winter, respectively. In both summer and winter, nitrogen-containing organic aerosols dominated the observed distribution of functionalized particle-phase species ionized by our analytical techniques, with 85% and 68% of

Deleted: Seasonal

Deleted: Indeed,

Deleted: w

Deleted: a mix of

Deleted: processing in summer

Deleted: in winter

30 total measured ion abundance containing a nitrogen atom, respectively. Nitrogen-containing

31 particles included reduced nitrogen functional groups (e.g., amines, imines, azoles) and common

32 NO_z contributors (e.g., organonitrates). The prevalence of reduced nitrogen functional groups

33 observed in the particle-phase, while frequently paired with oxygen-containing groups elsewhere

34 on the molecule, often rivaled that of oxidized nitrogen groups detected by our methods.

35 Supplemental gas-phase measurements, collected on adsorptive samplers and analyzed with a

36 novel liquid chromatography-based method, suggest that gas-phase reduced nitrogen compounds

37 are possible contributing precursors to the observed nitrogen-containing particles. Altogether,

38 this work highlights the prevalence of reduced nitrogen-containing compounds in the less-

39 studied Northeastern U.S., and potentially in other regions with similar anthropogenic, biogenic,

40 and marine source signatures.

42 **1. Introduction**

43 Coastal regions near the Long Island Sound often experience poor air quality due to a

44 combination of biogenic and anthropogenic emissions from upwind metropolitan areas along the

45 East Coast of the U.S. It is well established that these emissions undergo chemical

46 transformations to form secondary pollutants during hours to days of over-water transport to

47 downwind locations, including the states of Connecticut, Rhode Island, and Massachusetts (e.g.,

48 Cleveland et al., 1976). Emissions of gas-phase organic compounds (e.g., volatile, intermediate,

49 and semi-volatile organic compounds (VOCs, IVOCs, SVOCs)) and primary organic aerosols

50 (POA) are oxidized via numerous pathways in the atmosphere to yield ozone (O_3) and secondary

51 organic aerosol (SOA) (Hallquist et al., 2009). SOA constitutes a variable but significant fraction

52 of particulate matter with a diameter of 2.5 μm or less (i.e., $PM_{2.5}$). Both O_3 and $PM_{2.5}$ are of

54   particular concern for human health and climate; O_3 is known to cause an increase in respiratory-

55   related illnesses (Di et al., 2017; Jerrett et al., 2009), while $PM_{2.5}$ is known to cause adverse

56   cardiovascular, respiratory, and cognitive effects and to impact climate forcings (Di et al., 2017;

57   Hallquist et al., 2009; Kilian and Kitazawa, 2018; Pope and Dockery, 2006). Coupled with local

58   emissions and chemistry, these incoming aged air parcels from coastal metropolitan areas

59   contribute to the Long Island Sound region often entering nonattainment for O_3 (United States

60   Environmental Protection Agency, 2020), especially in the summer.

61   The chemistry and composition of organic compound emissions and secondary

62   transformation products in the Long Island Sound area is historically understudied, though some

63   past work has advanced our understanding of important sources and chemical pathways in the

64   region. For example, VOC and sub-micron particulate matter composition were investigated

65   during the 2002 New England Air Quality Study (de Gouw et al., 2005), with further VOC

66   speciation in 2004 during the New England Air Quality Study – Intercontinental Transport and

67   Chemical Transformation campaign (Warneke et al., 2007). More recently, a 2015 aircraft

68   campaign in the Northeast U.S. called WINTER characterized wintertime chemistry in the region

69   and also investigated organic aerosol formation via aerosol mass spectrometry (Schroder et al.,

70   2018). Finally, the LISTOS campaign in 2018 focused on measuring and modeling O_3 mixing

71   ratios over the Sound to investigate the dynamics of O_3 formation linked to large metropolitan

72   areas along the coast and associated downwind impacts (Zhang et al., 2020).

73   However, little is known about the molecular-level chemical composition of the gas-

74   phase I/SVOCs and functionalized organic aerosol formed in the Northeastern U.S. This

75   molecular-level speciation is key to understanding the physical/chemical properties of these

76   compounds in the atmosphere and their chemical transformations, especially for classes of

77   compounds containing reduced and oxidized nitrogen functional groups, whose emissions,

78   lifetime, and ultimate impacts are generally poorly understood. For example, nitrogen-containing

79   compounds that serve as reservoir species for nitrogen oxides may increase the overall lifetime

80   of nitrogen oxides in the atmosphere via renoxification mechanisms (e.g., the photolysis of

81   particulate nitrates, which has been studied in the marine boundary layer (Ye et al., 2016)); some

82   may act as light absorbing chromophores (e.g., the brown carbon studied from a methylglyoxal

83   and ammonium sulfate system, which yielded mostly N-containing chromophores (Lin et al.,

84   2015)); and some may have adverse, but uncertain, effects on human health (e.g., impacts on

85   immune response to allergens (Ng et al., 2017)).

86   There have been a wide range of measurements of organic nitrogen in the atmosphere,

87   and many past studies have emphasized enhancements in the contribution of this organic

88   nitrogen in various forms of water in the atmosphere such as cloud water, fog water, rain water,

89   and aerosol liquid water. For example, in cloud water, observations of important contributions

90   from nitrogen- and oxygen-containing organic compounds have been made using Fourier-

91   transform ion cyclotron resonance mass spectrometry (FT ICR-MS) (Zhao et al., 2013). Across

92   all the oxygenates (i.e., CHO), oxygen- and nitrogen-containing compounds (CHON), oxygen-

93   and sulfur-containing compounds (CHOS), and oxygen-, nitrogen-, and sulfur-containing

94   compounds (CHONS) that Zhao et al. (2013) observed in cloud water, roughly 65% of ions (by

95   number count) contained a nitrogen atom. Roughly half of all species observed were CHON

96   compounds. Also, roughly half of the CHON species had low O/C (<0.7), and were hypothesized

97   to contain reduced nitrogen functional groups. Another example from a study in the Southeastern

98   U.S. by Boone et al. (2015) showed that cloud water samples contained a large fraction of

99   nitrogenated species relative to aerosol-phase samples. From a combination of direct infusion

electrospray ionization and nanospray desorption electrospray ionization measurements with high resolution mass spectrometry, Boone et al. (2015) observed roughly four times more CHON molecular formulas in cloud water than in particle-phase samples, representing ~20% of all ions, by number count, in cloud water. They also suggested an important role for aqueous-phase reactions occurring between water-soluble oxygenated organic compounds and a diversity of nitrogen-containing species such as ammonium, nitrate, small amines, among others (Boone et al., 2015).

Similar observations have been made in fog water samples. For example, LeClair et al. (2012) discussed the importance of water-soluble organic nitrogen-containing compounds in fog water using FT ICR-MS. Roughly half of their observed compounds contained a nitrogen atom, and by tracking neutral losses, they identified that 50-83% of their observed CHON species showed a neutral loss of HNO_3 and thus likely contained a nitrate group. They noted that in the absence of HNO_3, CH_3NO_3, NO, or NO_2 losses, the remaining nitrogen-containing ions observed likely contained reduced nitrogen groups such as amine, amino, or imine structures (LeClair et al., 2012). Another study of fog droplets with aerosol mass spectrometry by Kim et al. (2019) showed an enrichment of organic nitrogen in fog droplets, including observations of reduced nitrogen groups such as imidazoles and pyrazines (Kim et al., 2019). They observed fog water's N/C ratio to be roughly 4 times greater than the N/C ratio in oxygenated organic aerosol samples.

These trends extend to rain water as well; FT ICR-MS measurements of rainwater in the Northeastern U.S. by Altieri et al. (2009) showed large contributions of nitrogen-containing organic compounds (Altieri et al., 2009). Approximately 70% of their observed nitrogen-containing species were CHON species from positive mode ionization, which they suggested consisted largely of reduced nitrogen functional groups based on their detection in positive

123   ionization mode and based on their elemental ratios. Similar enhancements in bulk organic

124   nitrogen, made by measuring total nitrogen content and subtracting the contribution from

125   inorganic nitrogen, were noted in both rain water and aerosols collected on the Mediterranean

126   coast (Mace et al., 2003a), and in both rain and cloud water in a Caribbean background marine

127   environment (Gioda et al., 2011).

128   While Boone et al. (2015) showed enhanced nitrogen content in cloud water relative to

129   aerosol particles, aerosol-phase samples have also been observed in other studies across the

130   globe to contain high organic nitrogen content. For example, at another location in the

131   Southeastern U.S. with strong marine and continental air influence, Lin et al. (2010) observed

132   that organic nitrogen in $PM_{2.5}$ contributed roughly 33% of total $PM_{2.5}$ nitrogen mass, which they

133   computed by subtracting inorganic nitrogen contributions from total nitrogen content, as

134   mentioned above (Lin et al., 2010). Similarly, 61% of primary marine aerosols (magnitude-

135   weighted) collected from a ship in the Atlantic ocean and analyzed by FT ICR-MS were shown

136   to contain nitrogen, and 54% of these primary marine aerosol species were CHON compounds,

137   with the remaining 7% of nitrogen content distributed across CHONS and CHONP species

138   (Wozniak et al., 2014). These primary marine aerosols typically had O/C ratios less than 0.5 and

139   were also likely reduced nitrogen-containing, consistent with Zhao et al. (2013). Other examples

140   include bulk organic nitrogen measurements from aerosols collected inland during both the wet

141   and dry seasons in the Amazon basin (Mace et al., 2003b), from aerosols sampled in Davis,

142   California (Zhang et al., 2002), and from aerosols (and fog) in the Po Valley in Italy (Montero-

143   Martínez et al., 2014).

144   Finally, a recent study of aerosols collected in a forest in Tokyo highlighted the role of

145   aerosol liquid water as another important medium for the formation of water soluble organic

146 nitrogen-containing species, and showed a positive correlation between the concentration of

147 aerosol liquid water and water-soluble organic nitrogen (Xu et al., 2020).

148   Considering the coastal nature of our Long Island Sound site and general prevalence of

149 water in the local/regional atmosphere (e.g., as cloud water, fog water, rain water, and aerosol

150 liquid water), the overall goal of this study was to examine the composition and contributions of

151 nitrogen-containing organic compounds from mixed anthropogenic, biogenic, and marine

152 sources, as well as the possible roles of secondary product formation via aqueous-phase

153 chemistry. We collected samples of organic gases and particles for detailed chemical speciation

154 on the coast of the Long Island Sound in Guilford, Connecticut. We note that we used this site as

155 a case study, but our observations of emissions and chemistry at this site are likely informative

156 for other coastal urban and downwind regions due to the ubiquity of nitrogen-containing

157 emissions from anthropogenic, biogenic, and marine sources.

158   Samples were collected during the summer and winter, and analyzed via high resolution

159 mass spectrometry to speciate the complex mixture of emissions and chemical transformation

160 products. These samples were taken alongside several targeted pollutant measurements including

161 O_3, nitrogen oxides (NO_x), particulate matter with a diameter of ≤ 2.5 μm ($PM_{2.5}$), and black

162 carbon (BC), all to inform our chemically-speciated analyses, and to contribute to a longer-term

163 characterization of this coastal area.

164   The specific objectives of this study were to: (1) investigate compositional differences

165 and possible chemical pathways contributing to measured summer and winter functionalized

166 organic aerosols at this site; (2) examine the relative contributions of reduced and oxidized

167 nitrogen groups to functionalized organic aerosol; and (3) use a novel sampling and liquid

168 chromatography-based analytical approach to probe the molecular-level composition of

175   functionalized gas-phase organic compounds and investigate possible nitrogen-containing gas-

176   phase precursors to the observed reduced nitrogen-containing particles.

177

178   **2. Materials and Methods**

179   We collected measurements at the Yale Coastal Field Station (YCFS) in Guilford,

180   Connecticut (41.26°N, 72.73°W) (Rogers et al., 2020). Inlets were positioned facing the Long

181   Island Sound (i.e., South-Southeast) to capture onshore flow. The YCFS often received aged

182   urban incoming air from East Coast metropolitan areas, similar to known common air parcel

183   trajectories in the region (Figure S1). However, due to extensive mixing in the Northeast corridor

184   and over the Long Island Sound, along with extended collection times for offline gas- and

185   particle-phase samples, we also observed considerable biogenic and anthropogenic influence

186   from other areas of the Northeastern U.S.

187

188   2.1. Offline Samples of Organic Particles and Gases Analyzed via Liquid and Gas

189   Chromatography with Mass Spectrometry

190   We discuss three types of sampling and quadrupole time-of-flight mass spectrometry-

191   based analyses here: particles collected on Teflon filters and analyzed using liquid

192   chromatography with electrospray ionization, gases collected on packed adsorbent tubes and

193   analyzed using gas chromatography with atmospheric pressure chemical ionization, and

194   functionalized gases collected on cooled polyether ether ketone (PEEK) samplers and analyzed

195   using liquid chromatography with electrospray ionization. Teflon filter and adsorbent tube

196   measurements were collected at the YCFS during the summer as part of the 2018 Long Island

197   Sound Tropospheric Ozone Study (LISTOS), from July 9 to August 29, 2018. Additional filter

Deleted:

199 and adsorbent tube samples were collected during the following winter from February 25 to

200 March 5, 2019. Supplemental wintertime gas-phase samples on PEEK tubing were collected

201 briefly from March 5-6 2020, prior to the COVID-19 shutdown. These sampling periods are

202 discussed here as summer and winter case studies but longer campaigns are warranted to assess

203 full seasonal trends.

204   A custom filter and adsorbent tube housing was constructed to simultaneously collect

205 particle- and gas-phase organic compounds, respectively (Sheu et al., 2018). The filter was

206 positioned immediately upstream of the adsorbent tube to collect particles for analysis and to

207 prevent particles from reaching the gas-phase adsorbent tube sample. The housing was designed

208 to minimize spacing between the filter and adsorbent tube to reduce gas-phase losses to upstream

209 surfaces, and was built out of a modified passivated stainless steel filter holder (Pall) and an

210 aluminum block with sealed 6.34 mm (1/4") holes for adsorbent tubes (Sheu et al., 2018).

211   For filter and adsorbent tube collection, we used a short inlet (0.9 m long, 5/8" OD

212 stainless steel tubing, positioned 2.5 m above the ground) upstream of the custom sampler to

213 allow the sampling media to be housed in an air-conditioned trailer. A stainless steel mesh screen

214 (84 mesh) was used at the opening of the inlet to limit particle size to $\sim PM_{10}$ and to prevent large

215 particles from entering the sampler (Ditto et al., 2018). Penetration efficiency through the mesh

216 screen was computed for the 20 L/min flow rate using the screen thickness, mesh size (84 mesh),

217 wire diameter, and accounting for the effects of diffusion, impaction, and interception. Based on

218 this modeling, we expect roughly 50% penetration efficiency at PM_{10} and 0% at PM_{11} and larger.

219

220

221

For filter and adsorbent tube collection, we used a short inlet (0.9 m long, 5/8" OD stainless steel tubing, positioned 2.5 m above the ground) upstream of the custom the sampler to allow the sampling media to be housed in an air-conditioned trailer. A stainless steel mesh screen (84 mesh) was used at the opening of the inlet to limit particle size to $\sim PM_{10}$ and to prevent large particles from entering the sampler (Ditto et al., 2018). P.

2.1.1. Filter sampling, analysis, and data QA/QC

Teflon filters (47 mm, 2.0 μm pores, Tisch Scientific) were used for particle-phase sampling. Filters were collected at 20 L/min for 8 hours, during the day (9:00am-5:00pm) and at night (9:00pm-5:00am). Samples were extracted in methanol and analyzed via liquid chromatography (LC) using an Agilent 1260 Infinity LC and an Agilent Poroshell 120 SB-Aq reverse phase column (2.1 x 50 mm, 2.7 μm particle size). The LC was coupled to an electrospray ionization (ESI) source and a high-resolution mass spectrometer (Agilent 6550 Q-TOF), and operated following previously described methods (Ditto et al., 2018, 2020). The mass resolution (M/ΔM) of the Q-TOF used in this work was ≥25,000-40,000, and the mass accuracy was 1-2 ppm. Our use of LC (or GC) to separate compounds prior to their ionization and detection by the mass spectrometer reduced mass spectral interferences and thus enabled accurate molecular formula assignments beyond what would be possible by relying on the Q-TOF's mass resolution alone.

Filter extracts were run with MS (i.e., TOF-only, to identify molecular formulas) and MS/MS (i.e., tandem mass spectrometry, to identify functional groups) data acquisition, using both positive and negative mode electrospray ionization. These methods are hereafter referred to as "LC-ESI-MS" and "LC-ESI-MS/MS", respectively. Acquisition and non-targeted analysis methods, including data quality assurance and quality control (QA/QC), are discussed in past work (Ditto et al., 2018, 2020). Briefly, for LC-ESI-MS analyses, any ion mass appearing in both a sample and its corresponding blank (matching ion mass with a tolerance of 5 ppm, and matching ion retention time with a tolerance of 0.25 min—both tolerances were chosen to be quite conservative) was removed if its abundance in the sample was less than 5 times its abundance in the blank. Ions with greater sample:blank ratios were retained, and the abundance

255 of the blank peaks were subtracted from the sample peaks. Positive and negative ionization mode

256 data were combined and any ions appearing in both modes were flagged; abundances were

257 averaged and the compound was only counted once. Ions from m/z 50-600 were assigned

258 formulas assuming hydrogen or sodium adducts in positive mode and acetate adducts or

259 deprotonation in negative mode. We also allowed for the neutral loss of water. Only peaks that

260 well-surpassed instrument noise and that had strong peak quality scores (based on both liquid

261 chromatography and mass spectrometry data) were selected for formula identification according

262 to thresholds detailed in Ditto et al. 2018. Formulas were assigned with the following elemental

263 constraints in Agilent's Mass Hunter software: $C_{3-60}H_{4-122}O_{0-20}N_{0-3}S_{0-3},$ minimizing the ppm

264 mass difference between the observed and proposed ion mass and accounting for isotope

265 distribution. Prior to non-targeted analysis, further QA/QC was performed on these formula

266 identifications using custom R code. As discussed by Kind and Fiehn (2007), the number of

267 elements was further constrained to 39 carbons and 72 hydrogens, and H/C ratios were checked

268 to ensure they fell within expected limits $(0.2 < H/C < 3.1)$ (Kind and Fiehn, 2007). Formulas

269 were then screened to ensure they agreed with the Nitrogen rule, to ensure that all double bond

270 equivalent values were integers, and to flag any large mass differences (>7 ppm) between the

271 observed and proposed mass for a given molecular formula.

272   For MS/MS, any ions from the LC-ESI-MS analyses that passed these QA/QC steps were

273 targeted for MS/MS fragmentation at 5, 10, 20, 30 and 40 V. We used SIRIUS with

274 CSI:FingerID for functional group identification with a subset of compounds from MS analysis

275 (Dührkop et al., 2015, 2019), as detailed in past work (Ditto et al., 2020). We assumed the same

276 ionization behavior as discussed above, with the same elemental composition constraints and a

277 conservative 7 ppm mass tolerance. Functional groups for the top-scoring candidate structure for

278 each ion were tallied with APRL Substructure Search Program (Ruggeri and Takahama, 2016).

279 The exact position of each functional group was not considered, as the focus of our work was

280 instead to assess the presence or absence of atmospherically relevant functional groups and their

281 combinations across a large number of multifunctional compounds.

282 After stringent QA/QC for peak shape and accurate molecular formula determination,

283 non-targeted compound identification from LC-ESI-MS identified an average of 200±56 and

284 167±47 compounds per sample analyzed in summer and winter, respectively, across 34 samples

285 in summer and 15 in winter.

286 We note that filter ion abundance data is presented as combined positive and negative

287 ionization mode data, which treats the compounds equally without corrections for ionization

288 efficiency. As mentioned above, compounds were not double counted; any ion appearing in both

289 positive and negative mode was flagged, its average abundance computed, and it was tallied only

290 once. While ionization efficiency differences between compound types exist, their exact effects

291 for multifunctional compounds present in a complex mixture are uncertain. Thus, similar to other

292 studies and to our past work, we treat the intercomparison across compounds without adjusting

293 for ionization efficiency differences (Ditto et al., 2018). We note that the figures in the main text

294 are displayed as fractions of total observed ion abundance, to consider variations in atmospheric

295 abundance across the complex mixture of functionalized species. However, due to uncertainty in

296 exact ionization efficiency, these are not intended to directly represent mass concentration. For

297 comparison, identical figures represented by occurrence (i.e., unweighted by abundance) are

298 presented in the SI (Figures S4-S6, S8-S9, S11, S13); general observations remain similar

299 between abundance weighted and occurrence results.

300

307 *2.1.2. Adsorbent tube sampling, analysis, and data QA/QC*

308   Gas-phase samples were collected on glass adsorbent tubes (6.35 mm OD, 88.9 mm long)

309   packed with quartz wool, glass beads, Tenax TA, and Carbopack X (Sheu et al., 2018). Samples

310   were collected at 200 mL/min for 2 hours, sub-sampling off of the 20 L/min filter flow, during

311   the day (2:00-4:00pm) and at night (2:00-4:00am). Adsorbent tubes were analyzed using a

312   GERSTEL TD3.5+ thermal desorption unit and an Agilent 7890B gas chromatograph (GC) with

313   a DB5-MS UI column (30 m x 320 μm x 0.25 μm). The GC was coupled to an atmospheric

314   pressure chemical ionization (APCI) source and the same Q-TOF as above, operated with MS

315   (i.e., TOF-only) data acquisition and positive ionization mode only. These methods are hereafter

316   called "GC-APCI-MS" and acquisition and analysis methods are discussed in past work (Ditto et

317   al., 2021; Khare et al., 2019). After QA/QC (as detailed in Section 2.1.1), this non-targeted

318   analysis yielded an average of 388±201 and 612±133 compounds per sample in summer and

319   winter, respectively, across 34 samples in summer and 14 samples in winter.

320

321 *2.1.1. PEEK collector sampling, analysis, and data QA/QC*

322   Finally, as a supplemental analysis to probe the composition of functionalized gases that

323   were not GC amenable and thus not measured using the adsorbent tube and thermal desorption-

324   gas chromatography techniques mentioned above, we used PEEK-based sample collectors and

325   liquid chromatography to trap and speciate oxygen-, nitrogen-, and/or sulfur-containing gases

326   without thermal desorption. This method was designed to target functionalized gases, which

327   represent important precursors, intermediates, and by-products in the atmospheric processing of

328   emitted organic compounds but are often challenging to speciate with traditional GC techniques

329   due to their chemical functionality, reactivity, and/or thermal lability. Additionally, in many gas-

330 phase measurement systems, primary emissions (i.e., hydrocarbons) can overwhelm the signal of

331 more functionalized analytes, adding to the challenge of speciating these lower abundance

332 compounds.

333   Thus, to probe the chemical composition of these functionalized gases, we used a

334 sampling approach, desorption method, separation method, and ionization technique that

335 leveraged their relatively lower volatility and higher polarity. This included adsorptive sampling

336 onto cooled PEEK tubing followed by direct inline desorption into the LC mobile phase for LC-

337 ESI-MS analysis. ESI was specifically chosen here because it is sensitive to functionalized

338 compounds. Testing was performed in positive and negative ionization mode, but field samples

339 were run in positive mode only. Further details and discussion of this method, including method

340 development and evaluation, can be found in Section S1 and Tables S1-3. Briefly, PEEK tubing

341 was cooled to 2°C and used as an adsorptive collector, with a Teflon filter positioned upstream

342 of the PEEK tubing to remove particles. PEEK was selected due to its inert behavior, thus

343 reducing the possibility for surface-analyte interactions that might inhibit effective inline solvent

344 desorption and dissolution. PEEK is also compatible with the solvents used in the LC system,

345 and is frequently used in LC instruments. Field samples were collected on cooled PEEK tubing

346 during the subsequent winter (March 5-6, 2020), for 2 hours each between 8:00am-2:00pm. For

347 these 2 hour (~2.6 L) field samples, functionalized gases in a typical 100-250 g/mol molecular

348 weight range were resolvable at ~25-60 ppt in the atmosphere, based on instrument detection

349 limits (Ditto et al., 2018). For analysis, each PEEK collector was installed in the LC system flow

350 path, and analytes were directly desorbed using the LC mobile phase solvents then trapped and

351 focused on the LC column for 20 minutes, before being analyzed using the same LC-ESI-MS

352 system in positive ionization mode (Figure 1). This inline mobile phase desorption step gently

356 mobilized potentially fragile analytes from the PEEK collector and trapped and focused them on
357 the LC column prior to chromatographic separation and mass spectral analysis. Additionally, this
358 preconcentration step allows for the detection and characterization of lower concentration
359 species. Data were processed and QA/QC were performed as detailed in Section 2.1.1.
360   We note that there are other existing approaches for offline collection of highly-
361 functionalized organic gases and particles that are compatible with LC analysis such as spray
362 chambers, particle into liquid samplers, coated denuders, PUF sampling, and more. This PEEK
363 sampling method with inline desorption into the LC mobile phase was pursued to reduce sample
364 preparation steps and thus possibilities for losses (e.g., during solvent extraction or evaporative
365 preconcentration), as well as for its direct similarity to the filter-based particle-phase LC-ESI-MS
366 analysis.
367   We also note that for all filter collection and LC analyses (filters and PEEK collectors), it
368 is possible that some functional groups of interest may have undergone hydrolysis on the filter
369 during 8-hour filter collection periods or in the LC mobile phase, which was primarily water at
370 the beginning of the LC solvent gradient. For example, organonitrates may be susceptible to
371 hydrolysis depending on their structure; tertiary organonitrates can undergo hydrolysis on the
372 timescale of minutes-hours depending on pH, while primary/secondary organonitrates are
373 relatively stable. Hydrolysis occurs more quickly at low pH. The pH of the LC mobile phase (pH
374 $\sim$ 2) and the pH of the sampled aerosol (pH < ~5, (Pye et al., 2020)) are both acidic; alpha-
375 pinene-derived organonitrates, for example, could have a lifetime of as low as of roughly 8
376 minutes to 1.5 hours across this pH range (Rindelaub et al., 2016). If hydrolysis occurred, some
377 of the observed compounds could be byproducts of other functionalized species. While we did

Deleted: (e.g. organonitrates)

Deleted:

Deleted: so

Deleted: , though this would require hydrolysis to occur on the order of a few minutes

383   not observe any of our nitrogen-containing test standards to hydrolyze over these timescales,

384   standards were not available to reflect every functional group observed in these datasets.

385

386   2.2. Supporting Measurements

387   O_3, NO_x, $PM_{2.5}$, and BC concentrations were recorded concurrently during both summer

388   and winter sampling periods. O_3 was measured with a 2B Tech Model 202 Ozone Monitor, NO_x

389   with a Thermo Scientific Model 42i-TL Analyzer, $PM_{2.5}$ with a MetOne BAM-1020 instrument,

390   and BC with a Magee Scientific AE33 Aethalometer. O_3 and NO_x inlets were constructed of FEP

391   tubing (1/4" OD), with a Teflon filter housed in a PFA filter holder upstream to remove particles.

392   The $PM_{2.5}$ inlet was made of stainless steel tubing (1 ¼" OD) and the BC inlet was made of

393   copper tubing (3/8" OD). Both particle inlets were outfitted with a $PM_{2.5}$ cyclone to limit particle

394   size to 2.5 μm and below.

395   All inlets were mounted 3 m above the ground. Instrument flow rates were calibrated

396   with an external mass flow controller. O_3 and NO_x monitors were zeroed with laboratory-

397   generated zero air. The O_3 monitor was calibrated against Connecticut Department of Energy and

398   Environmental Protection instrumentation and further confirmed with an O_3 generator in the lab.

399   The NO_x monitor was calibrated using a NO standard (AirGas, 2 ppm NO in nitrogen, ± 5%)

400   diluted to 25 ppb with laboratory-generated nitrogen gas. The BC instrument was programmed to

401   conduct an automatic performance check using particle-free air and the $PM_{2.5}$ instrument was

402   zeroed following MetOne protocols with particle-free air. O_3 and NO_x data were collected at 1-

403   second intervals, BC data were collected at 1-minute intervals, and $PM_{2.5}$ data were collected at

404   1-hour intervals. BC data were saved directly from the instrument, while O_3, NO_x, and $PM_{2.5}$

405   data were recorded with a LabJack T7 datalogger and custom LabView code. In addition, hourly

406   weather data (temperature, relative humidity, wind speed, wind direction) were collected with a

407   WeatherHawk weather station on top of the 3 m tower.

408   During the summer, we also collected a small number of size-resolved particle samples

409   on quartz filters using an eight-stage cascade impactor (Thermo Scientific Andersen Non-Viable

410   Cascade Impactor). Sizes ranged from 0.43-10.0 μm (stage 0: 9.0-10.0 μm, stage 1: 5.8-9.0 μm,

411   stage 2: 4.7-5.8 μm, stage 3: 3.3-4.7 μm, stage 4: 2.1-3.3 μm, stage 5: 1.1-2.2 μm, stage 6: 0.65-

412   1.1 μm, stage 7: 0.43-0.65 μm). Quartz filters were extracted and analyzed following the same

413   procedure as the Teflon filters discussed above, with the addition of a syringe filtration step to

414   remove insoluble fibers. The cascade impactor was positioned on the roof of the trailer and

415   pulled 28.3 L/min (GAST 1531-107B-G557X pump) through the inlet for periods of 8 hours

416   during the day and at night (same timing as above).

417   Finally, we computed 48-hour backward trajectories for every hour during each offline

418   sample collection period with the HYSPLIT Backward Trajectory Model (accessed online at

419   https://www.ready.noaa.gov/HYSPLIT.php), using GDAS1.0 meteorological data, the field site's

420   coordinates as each trajectory's end point, and a final trajectory height of 50 m above the

421   ground. We selected 48 hours trajectories to focus on regional influence at the site, and we

422   selected a final height of 50 m to be high enough to focus on the overall 48-hour dynamics and

423   reduce the possible influence of surface topography. Contributions from air parcels extending

424   beyond 48 hours likely exist, but are outside of the regional scope of our study.

425
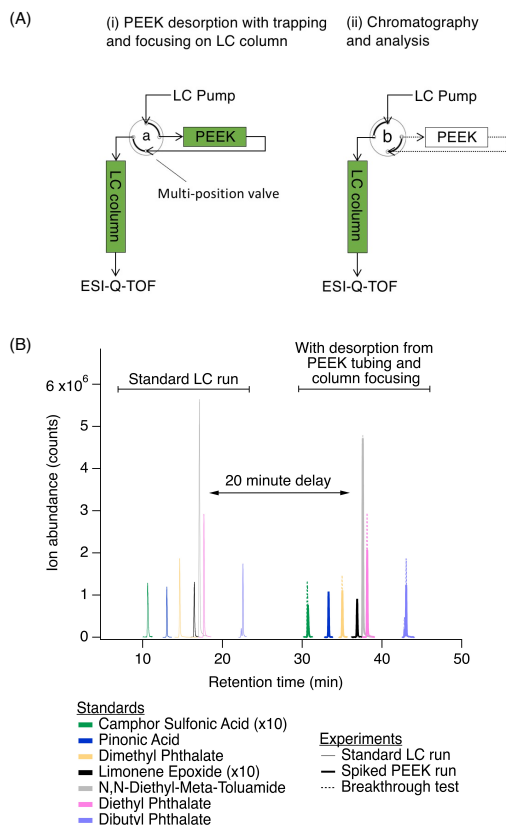
Figure 1. (A) Simplified analytical system setup for functionalized gas-phase compounds,
showing (i) desorption from the PEEK collector and trapping on the LC column in order to focus
analytes prior to chromatographic separation, and (ii) subsequent chromatographic separation
and analysis (discussed in detail in Section S1). Green shading indicates active solvent flow
through PEEK collector and/or LC column. A multi-position valve was switched from position
"a" (panel (Ai)) to position "b" (panel (Aii)) to remove the PEEK collector from the flow path
for chromatography and analysis. Table S1 describes the flow rates and solvents used in each of
these steps. (B) Comparison of select peaks from a typical LC run (solid traces from 10-23 min)
to that from a PEEK collector spiked with a standard (bold traces from 30-43 min) demonstrates
desorption, trapping/focusing, and similar chromatography. Comparable results from a 2-hour
breakthrough test at 2°C with 22 mL/min air flow are also shown (overlayed dotted traces from
30-43 min). Spiked PEEK and breakthrough tests were performed to validate this sampling and
analysis methods, and are discussed further in Section S1. Test analytes were used across a range
of functionality, with examples shown here and the full list in Table S2.

3. Results and Discussion

3.1. Characteristics of the Urban Regional Site

Backward trajectories for summertime and wintertime samples showed a strong urban influence. Summertime trajectories ranged from the northwest, west, and especially the southwest (i.e., New York City and other coastal metropolitan areas, similar to well-established and expected air flow patterns near the Long Island Sound). In contrast, trajectories were almost exclusively from the northwest in the winter (Figure S1). These air parcels brought a range of compounds from a mixture of anthropogenic, biogenic, and marine sources to the site, all with differences in gas- and particle-phase source profiles. However, due to the varied backward trajectories, dynamic variations in wind direction over the long duration filter samples (Figure S2), and a high degree of mixing over the Sound, our 8-hour samples are representative of mixed regional conditions in summer and winter, and are thus discussed in this context. Further detailed site characterization can be found in Section S2 and Figures S1-S3.

3.2. Summer and Winter Comparisons of Functionalized Organic Aerosols

3.2.1. Summertime composition and the influence of photochemistry and NO$_x$

During this period of active photochemistry, the observed distribution of particle-phase compounds in summertime samples spanned across the intermediate volatility (IVOC) to ultralow volatility organic compound (ULVOC) range, with a predominance of semivolatile (SVOC), low volatility (LVOC), and extremely low volatility organic compounds (ELVOC) as shown in Figure 2A as a function of compound class. To assess differences in summer and winter volatility distributions, we used individual molecular formulas and the Li et al. (2016) parameterization to estimate the saturation mass concentration ($\log(C_0)$) of each observed

465 compound (Li et al., 2016). Compounds were then classified into volatility bins following these

466 definitions: $VOC > 3*10^6$ µg/m^3; $3*10^6$ µg/m^3 > IVOC ≥ 300 µg/m^3; 300 µg/m^3 > SVOC ≥ 0.3

467 µg/m^3; 0.3 µg/m^3 > LVOC ≥ $3*10^{-5}$ µg/m^3; $3*10^{-5}$ µg/m^3 > ELVOC ≥ $3*10^{-9}$ µg/m^3; $3*10^{-9}$

468 µg/m^3 > ULVOC (Donahue et al., 2011; Schervish and Donahue, 2020).

469   Due to elevated summertime O_3 mixing ratios at the site (shown in Figure S3, 8-hour

470 maximum mixing ratio in summer: 57 ± 20 ppb, vs. winter: 46 ± 5 ppb, including day and night

471 sampling periods), O_3 may have influenced the photochemical processing of emitted volatile

472 species, especially unsaturated biogenic VOCs which readily undergo ozonolysis due to their

473 chemical structure. However, we did not observe a correlation between 8-hour maximum (or 8-

474 hour average) O_3 mixing ratios with average particle-phase volatility (as saturation mass

475 concentration), carbon number, or O/C (nor did we observe such relationships for gas-phase

476 organic compounds). There were, however, weak relationships between NO_x mixing ratios and

477 each of these particle-phase characteristics in the summer. While average NO_x mixing ratios

478 were slightly lower during the summer (as shown in Figure S3, 2.3 ± 1.5 ppb in summer vs. $3.7 \pm$

479 2.7 ppb in winter), NO_x mixing ratios trended weakly with particle-phase O/C ($r \sim 0.45$),

480 volatility (as saturation mass concentration, $r \sim 0.49$), and inversely with carbon number ($r \sim -$

481 0.56) in summer.

482   While our correlations and conclusions are somewhat limited by the 8-hour filter

483 sampling duration and the resulting highly regionally-mixed samples, one possible hypothesis is

484 that the presence of NO_x could have promoted more fragmentation reactions in the gas-phase

485 (Loza et al., 2014) that decreased average carbon number, and correspondingly increased

486 volatility and O/C. In fact, we observed highly oxidized C_3-C_6 compounds in the gas-phase (from

487 adsorbent tube measurements with GC-APCI (Section S2)) that were possibly products of these

493 fragmentation reactions of larger compounds. These trends of NO_x mixing ratios with O/C,

494 volatility, and carbon number were not apparent for the observed complex mixture of gas-phase

495 organic compounds. However, these highly oxidized gases may not have persisted in the gas-

496 phase and could have been taken up by the condensed/aqueous phase due to their water

497 solubility, where they would have instead contributed to the observed trends of NO_x with carbon

498 number, volatility, and O/C in the particle-phase. We note that if there was significant uptake of

499 gas-phase NO_z to the particle-phase, this may have in part contributed to the particle-phase

500 correlations with NO_x given that the chemiluminescence NO_x analyzer used in this study is

501 known to also respond to gas-phase NO_z (Dunlea et al., 2007).

502   Additionally, NO_x could have been involved in heterogeneous chemistry, promoting

503 oxidation and/or nitrogen addition reactions, such as interaction with $NO_3^{\bullet}$ to yield organonitrates

504 (Lim et al., 2016), formation and interaction with HONO to yield nitrophenols (Vidović et al.,

505 2018), or other pathways.

506

507 *3.2.2. Comparison to wintertime composition and the role of aqueous-phase chemistry*

508   In the winter, these same relationships between NO_x and particle-phase characteristics

509 were not observed. This is possibly due to the decreased role of photochemistry in the winter and

510 the increased role of other competing physical and chemical processes, such as aqueous-phase

511 chemistry. In the discussion of our results, we note that aqueous-phase chemistry is meant to be

512 inclusive of aqueous processing in aerosols, in cloud water, and/or in fog water, all of which may

513 have occurred upwind of the site during the 8 hour sampling periods under variable local and

514 regional weather conditions.

Deleted: with variations in weather conditions

516   In the winter, we observed a generally higher average saturation mass concentration
517 (summer: $\log(C_0)$ = -3.7 ± 3.9 μg/m^3, vs. winter: $\log(C_0)$ = -0.7 ± 4.0 μg/m^3). We note that this
518 comparison of saturation mass concentrations was performed at a reference temperature of 300
519 K, and we discuss the expected wintertime volatility shift below. The wintertime O/C was also
520 slightly lower than summer (summer: O/C = 0.5 ± 0.4 vs. winter: O/C = 0.4 ± 0.4). In the winter,
521 the observed chemical composition of the particle phase—both in terms of volatility and
522 functional group distribution— suggests a relatively greater role for aqueous-phase processing.
523 Our observations were similar to those made in past studies of higher volatility products from
524 fragmentation reactions in the aqueous phase (e.g., Brege at al., where they observed that aged
525 fog-water samples contained organic compounds with smaller carbon backbone structures than
526 non-aqueous aged particles, and linked this difference to aqueous-phase fragmentation reactions,
527 the uptake of smaller water-soluble gases to the aqueous-phase, and/or less oligomerization
528 (Brege et al., 2018); Yu et al., which discussed the role of fragmentation in aging aqueous
529 phenolic secondary organic aerosol (Yu et al., 2016); and Schurman et al., which discussed the
530 role of fragmentation and evaporation in cloud water (Schurman et al., 2018)). Similarly, here we
531 observed a shifted compound distribution that included smaller molecular weight and generally
532 higher volatility particle-phase species in winter compared to summer, along with notably
533 different functional group distribution, both of which could be attributed to aqueous chemistry.
534   We note that for direct comparison, volatility bins in Figure 2A-B were defined for the
535 same reference temperature (i.e., 300 K, the average summertime sampling period temperature),
536 though wintertime saturation mass concentrations for the observed compounds would shift
537 approximately 2 orders of magnitude lower due to lower temperatures (i.e., 270 K). The dotted
538 black line in Figure 2B shows the shift in bins expected at 270 K. In the winter, compounds

565 defined IVOCs or SVOCs at 300 K will expectedly exhibit a greater degree of partitioning to the

566 particle phase, though the effect of this temperature shift on partitioning was likely more

567 pronounced for the SVOCs than IVOCs (Table S4). Even when accounting for this shift, the

568 mean saturation mass concentration of wintertime samples was $\log(C_0) = -2.7 \pm 3.9$ μg/m^3,

569 which is still higher than the mean summertime saturation mass concentration of $\log(C_0) = 3.7 \pm$

570 3.9 μg/m^3 and thus still demonstrates a volatility difference between summer and winter, with

571 higher volatility species in winter. This shift is also reflected in the carbon number distribution

572 observed via the LC-ESI-MS/MS analysis of this sample set shown in Ditto et al., (2020), Figure

573 S5. In addition to this shift in molecular size and volatility, there was a distinct change functional

574 group composition from summer to winter, discussed below.

575   To assess the potential contribution of aqueous-phase chemistry, we also estimated

576 aerosol liquid water concentrations based on available data in Section S2.1. We estimated a

577 lower but still appreciable aerosol liquid water content in winter relative to summer, but with

578 fewer photochemical processes in winter along with generally cloudier/foggier local weather

579 (i.e., 44% of summer sampling periods with partly cloudy or cloudy weather conditions vs. 67%

580 of winter sampling periods, from Weather Underground archive), aqueous-phase processing

581 likely remains an important pathway. We note that the compounds discussed here could have

582 been formed locally or regionally, and thus the role of conditions at the site (aerosol liquid water,

583 cloud cover, fog cover) is just as important as the conditions in the surrounding upwind region.

584 As a result, it is challenging to pinpoint the exact contributions of aerosol liquid water, in-cloud,

585 or in-fog processing, and we consider that all three may be occurring upwind or near the site.

586   Furthermore, from MS/MS analysis, we observed functional groups that were possible

587 indicators of aqueous-phase processing, including the presence of nitrophenols during the winter,

588 which may have formed via dark aqueous-phase reactions with HONO (Vidović et al., 2018),

589 and relatively low contributions from carbonyls across seasons, possibly linked to carbonyl

590 hydrolysis (Ditto et al., 2020). Based on laboratory studies, the presence of azole functional

591 groups and other heterocyclic nitrogen species could also indicate aqueous phase processing, and

592 may be formed from small carbonyl precursors such as glyoxal (DeHaan et al., 2009; Grace et

593 al., 2019) and biacetyl (Grace et al., 2020) reacting with atmospheric ammonia or small amines.

594 Many of the N-only containing azoles observed here had similar substructures to those formed in

595 the aqueous-phase reactions of small carbonyls with ammonia/amines (DeHaan et al., 2009;

596 Grace et al., 2019). In addition, as discussed above, we observed many small gas-phase C_3-C_6

597 compounds at the site in the summer, which likely included multifunctional isoprene oxidation

598 products (e.g., glycoaldehyde, hydroxyacetone, and isomers); these potential precursors could

599 have reacted with atmospheric ammonia or species containing amino groups to form the

600 observed azole-containing reaction products. We observed more azoles during the summer (Ditto

601 et al., 2020), perhaps due to the increased prevalence of the C_3-C_6 precursors and overall

602 prominence of atmospheric water (e.g., aerosol liquid water, cloud water, fog water).

603   Lastly, the role of aqueous-phase chemistry in the region is further supported by prior

604 summertime observations at Brookhaven National Laboratory (on the opposite side of the Long

605 Island Sound), which examined a low-volatility oxygenated organic aerosol factor in the source

606 apportionment of aerosol mass spectrometry measurements, and showed a strong contribution

607 from carboxylic acids and other ELVOCs that were attributed to aqueous-phase processing

608 (Zhou et al., 2016).
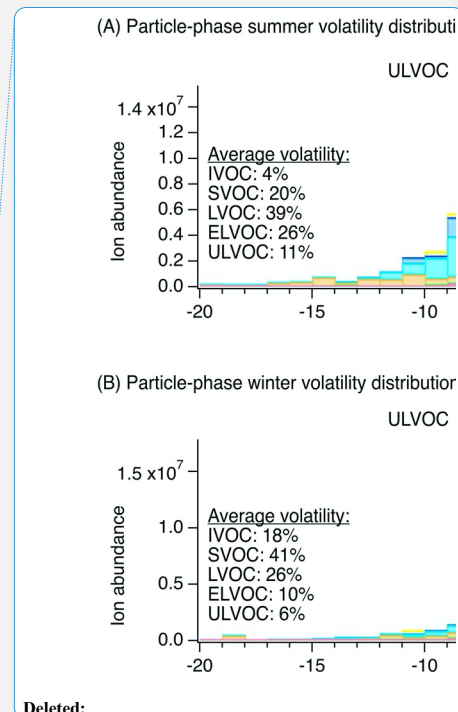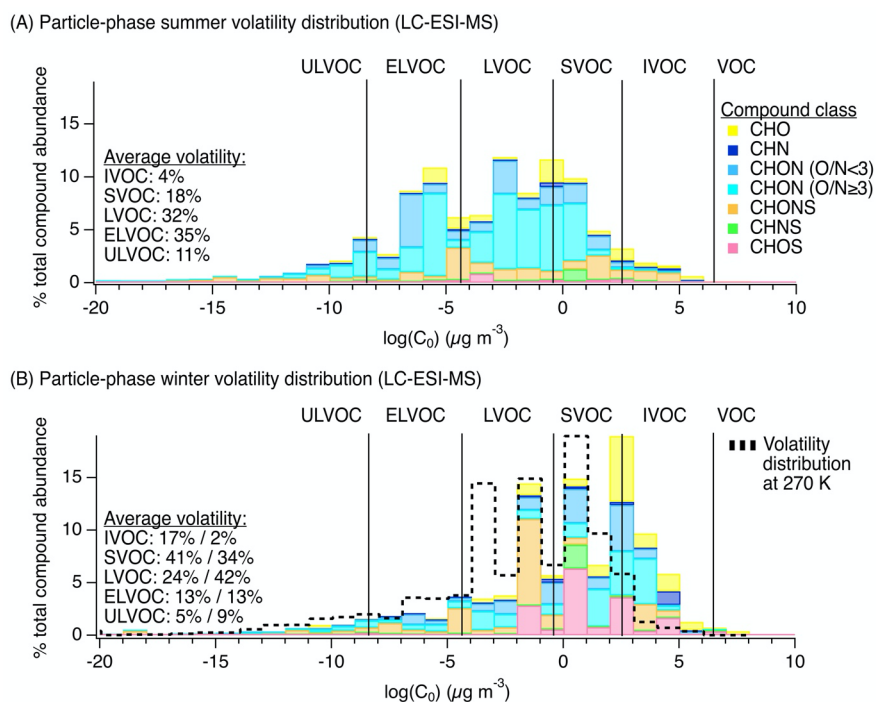
610

Figure 2. Chemical composition of particle-phase organic compound mixtures at the YCFS from LC-ESI-MS measurements. (A) and (B) show particle-phase volatility distributions by compound class in the summer (N=34) and winter (N=15), respectively, weighted by ion abundance. The same data tallied by occurrence are shown in Figure S4 for comparison. For direct comparison, volatility bins were defined for the same reference temperature in (A) and (B) (i.e., 300 K, the average summertime sampling period temperature), though wintertime saturation mass concentrations for the observed compounds would shift approximately 2 orders of magnitude lower due to lower temperatures (i.e., 270K). The dotted black line in (B) shows the shift in bins expected at 270 K, described further in Table S4. The average volatility distributions listed in (B) are shown at 300 K (%) followed by the estimate at 270 K (%).

3.2.3. Comparison to other sites using the same sampling and analytical methods

The distribution of compound classes observed at the YCFS was significantly different

from observations at a range of field sites discussed in past studies (Figure 3), including a remote

forested site (i.e., the PROPHET site in Northern Michigan), an urban inland site (i.e., near

634 downtown Atlanta) across two seasons, and in New York City (Ditto et al., 2018, 2019). We

635 perform a direct comparison to our past studies here, because the same sampling and analytical

636 methods were used, thus we can compare the distribution of ions observed without any biases

637 due to differences and uncertainties resulting from variations in sampling or ionization chemistry

638 between instruments. While a more detailed site-to-site comparison is outside the scope of this

639 work, the proximity of the YCFS to the ocean and thus the impact of marine emissions and over-

640 water chemistry likely contributed to the differences between the YCFS and inland locations. In

641 particular, at the YCFS, we observed notably smaller relative contributions from compounds

642 containing carbon, hydrogen, and oxygen (i.e., CHO, 11-16% of observed functionalized

643 compounds here vs. 34-50% at other sites), and the contributions from nitrogen-containing

644 particle-phase compounds at the YCFS were in stark contrast to other sites. Here, 85% of

645 compounds (by ion abundance) in summer and 68% of compounds in winter contained at least

646 one nitrogen atom, compared to 38-51% at the other previously studied sites (Figure 3). These

647 nitrogen-containing species were comprised of compounds with various reduced and oxidized

648 nitrogen-containing functional groups with varying oxygen-to-nitrogen ratios (O/N), which are

649 broadly classified and discussed below as compounds containing carbon, hydrogen, and nitrogen

650 (i.e., CHN), and compounds containing carbon, hydrogen, oxygen, and nitrogen (i.e., CHON

651 (O/N ratio < 3), and CHON (O/N ratio $\geq$ 3)). There were notably greater contributions at the site

652 from nitrogen-containing compounds that also contained at least one oxygen atom, including

653 CHON compounds with O/N < 3 (19-20% here vs. 10-15% at other sites), CHON compounds

654 with O/N $\geq$ 3 (24-44% here vs. 14-19% at other sites), as well as compounds containing oxygen,

655 nitrogen, and sulfur (i.e., CHONS, 20-21% here vs. 9-10% at other sites) (Ditto et al., 2018).

658   We note that while these measurements were of PM_{10} aerosols, the observations of high

659   nitrogen content were not biased by the inclusion of larger, primary (possibly biological)

660   particles. Quartz filter samples collected with a cascade impactor at the site during the summer

661   and analyzed with the same LC-ESI-MS methods did not show any significant differences

662   between any of these nitrogen-containing compound classes as a function of particle size, across

663   particles ranging from 0.4 to 10 μm (i.e., 69%-71% of ion abundance for PM ≤ 2.2 μm and 69%-

664   73% of ion abundance for PM ranging from 2.2-10 μm were nitrogen-containing species,

665   summarized in Table S5). This is consistent with past studies which have demonstrated that

666   amines, as one example of a prominent nitrogen-containing functional group, are ubiquitous in

667   size-resolved aerosol samples in urban and rural locations (VandenBoer et al., 2011).

668   The prevalence of nitrogen-containing species at the YCFS is consistent with the study at

669   Brookhaven National Laboratory discussed above, where a dedicated nitrogen-enriched aerosol

670   mass spectrometry factor was identified, and contained prevalent signal from aliphatic amines

671   and amides. However, in the Brookhaven study, the nitrogen-enriched factor was associated with

672   industrial amine emissions that were enhanced during periods of south/southwestern backward

673   trajectory influence, and that had correlations with tracers linked to industrial processes. In our

674   study, there was no correlation between backward trajectory direction and the contribution of

675   nitrogen-containing species. Also, wintertime air parcels arrived predominantly from directions

676   other than south/southwest, suggesting that the nitrogen-containing species observed in our study

677   were the result of mixed anthropogenic, biogenic, and marine precursors and their transformation

678   products. This high nitrogen content at the YCFS, where aqueous-phase chemistry is expected to

679   be important, is also consistent with the cloud water composition discussed in Zhao et al. (2013),

680   which reported roughly 65% of detected ions in their cloud water samples to contain a nitrogen

Deleted: were

Deleted: measurements

Deleted: possibly

Deleted: statistically

Deleted: .

Deleted: as an example of reduced nitrogen

687   atom, and the primary marine aerosol composition discussed in Wozniak et al. (2014), where

688   61% of their observed compounds contained nitrogen and 54% were CHON species.
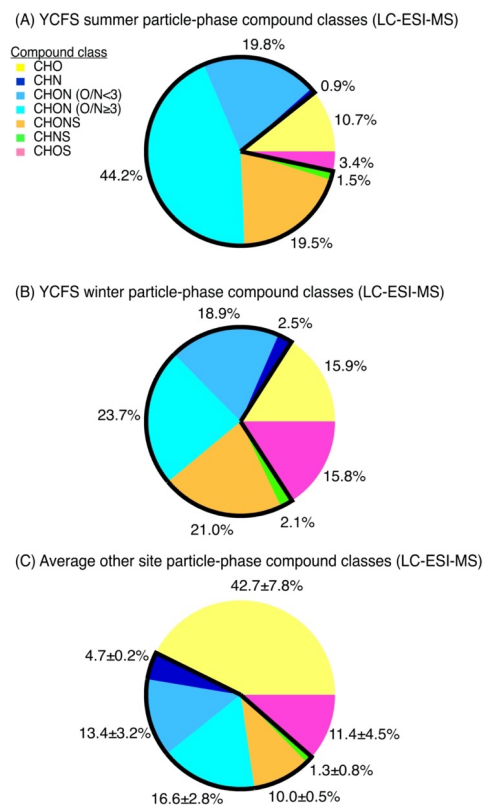
689
690 **Figure 3.** Particle-phase compound class distributions shown as fractions of total detected ion
691 signal in the (A) summer and (B) winter at the YCFS, weighted by compound abundance, in
692 contrast with (C) the average compound class distribution from previously studied forested,
693 urban inland, and urban coastal sites. The sites selected for comparison in (C) were chosen
694 because the same sampling and analysis methods were used. Nitrogen-containing compound
695 class contributions are outlined in black, and are notably larger at the coastal site compared to
696 other sites studied with these same filter collection and analysis methods. We note that while a
697 significant fraction of species contained nitrogen, individual compounds contained 1-3 nitrogen
698 atoms and the majority of the ion's molecular mass consisted of carbon and hydrogen atoms
699 (mean N/C in summer: 0.13 ± 0.1, mean N/C in winter: 0.22 ± 0.19 for all N-containing ions).
700 Note: CH and CHS species have poor ESI ionization efficiencies and are thus excluded here.
701 Data tallied by occurrence are shown in Figure S5 for comparison.

708   3.3. Speciating Particle-Phase Multifunctional Nitrogen-Containing Compounds

709   The observed particle-phase species were highly functionalized, often multi-functional,

710   and contained combinations of oxygen, nitrogen, and/or sulfur heteroatoms. Here, we discuss the

711   functional groups present, broken up by the nitrogen-containing compound classes shown in

712   Figures 2-3, with additional discussion of other relevant compound classes in Section S3.

713

714   *3.3.1. CHN compounds*

715   While nitrogen-containing compounds in general were very prominent at the site (Figure

716   3A-B), CHN compounds were relatively less abundant in these samples of functionalized

717   organic aerosol. Particle-phase CHN compounds represented just 1% and 3% of observed

718   functionalized organic aerosol abundance in summer and winter, respectively, which was similar

719   to observations at other ambient sites (~5% CHN) (Ditto et al., 2018).

720   In the summertime LC-ESI-MS/MS measurements, CHN particle-phase compounds were

721   comprised primarily of amines (72% of CHN species contained an amine group) and nitriles

722   (28% of CHN species contained a nitrile group), as shown in Figure 4. In the winter, these

723   compounds were nearly exclusively amines (present in 99% of CHN species). Amines have

724   many primary land-based sources (e.g., biogenic emissions (Kieloaho et al., 2013), agricultural

725   activity (Ge et al., 2011), emissions from decomposing organic matter (Ge et al., 2011;

726   Sintermann and Neftel, 2015), biomass burning (Ge et al., 2011), emissions from port activity

727   (Gaston et al., 2013), chemical products (Khare and Gentner, 2018), and vehicle exhaust

728   (Sodeman et al., 2005)), but their presence on the coast could also indicate marine contributions.

729   Amines have been detected both in bulk ocean water, the surface microlayer, and in sea spray

730   aerosol, and their emissions and chemical transformations in the marine environment have been

731   the topic of many recent studies (e.g., Brean et al., 2021; Dall'Osto et al., 2019; Decesari et al.,

732   2020; Di Lorenzo et al., 2018; van Pinxteren et al., 2012, 2019; Quinn et al., 2015; Wu et al.,

733   2020). In the summer, biogenic and marine sources likely dominated the amine distribution,

734   while in the winter, anthropogenic amine sources likely became more important.

735   Recent studies have also evaluated amine phase partitioning or formation in cloud/flog

736   water (e.g., Chen et al., 2018; Youn et al., 2015), as well as condensed-phase or aqueous-phase

737   pathways that may transform emitted amines (e.g., Ge et al., 2016; Lim et al., 2019; Tao et al.,

738   2021). Interestingly, the observed amines at this site, as well as other reduced nitrogen groups

739   like nitriles, imines, and enamines, were not present exclusively in CHN species and thus were a

740   mix of both direct emissions and chemically processed compounds. Reduced nitrogen groups

741   were often paired with hydroxyl groups, carboxylic acids, carbonyls, ethers, and esters as part of

742   nitrogen and oxygen containing compounds with a range of O/N ratios. This is consistent with

743   other studies observing reduced-nitrogen contributions to CHON compound classes, such as

744   Zhao et al. (2013), LeClair et al. (2012), and Altieri et al (2009), discussed above. As such, we

745   discuss CHON species as a function of O/N ratio to focus on differences between less-

746   oxygenated (O/N < 3) and more-oxygenated (O/N $\geq$ 3, e.g., organonitrates) species, using a ratio

747   of 3 to distinguish between the two as informed by the O/N ratio of the organonitrate functional

748   group.

749

750   *3.3.2. CHON (O/N < 3) compounds*

751   CHON (O/N < 3) compounds were notably more important at this site than other sites,

752   representing 20% and 19% of observed functionalized organic aerosol abundance in summer and

753   winter, respectively (Figure 3A-B), compared to ~13% at other sites (from predominantly

754 summer measurements). These CHON compounds included some functional groups that

755 contained both oxygen and nitrogen, such as amide groups (12% of this compound class's

756 nitrogen content in summer, vs. 1% in winter, Figure 4) and nitro groups (15% of this nitrogen

757 content in summer, vs. 6% in winter, Figure 4). However, most CHON (O/N < 3) compounds

758 were comprised of a combination of nitrogen- *or* oxygen-containing groups, rather than a

759 functional group containing both nitrogen and oxygen. This included large contributions from

760 hydroxyls and ethers across both seasons, as well as important contributions from amines,

761 isocyanates, and heterocyclic nitrogen, as shown in Ditto et al., 2020 (Figure 1). The presence of

762 these functional groups in the winter could be indicative of wood burning emissions in the

763 region, which has been observed in the wintertime in past ambient sampling in the Northeast

764 U.S. (Sullivan et al., 2019). Isocyanates contributed notably to this compound class during the

765 winter, which could similarly be linked to burning wood, other biomass, building materials

766 (Leslie et al., 2019; Priestley et al., 2018; Roberts et al., 2014), or could be photochemically

767 produced via the oxidation of amines and amides (Borduas et al., 2015; Leslie et al., 2019).

768 Importantly, levoglucosan, a common biomass burning tracer, was observed across nearly all

769 daytime and nighttime winter particle-phase samples (verified with an authentic standard),

770 supporting the influence of biomass burning compounds at the site. Together, the overall high

771 prevalence of reduced nitrogen at this site could be influenced by the mixing of aged biomass

772 burning plumes with marine air, which is consistent with past observations of very high

773 alkylamine concentrations in biomass burning particles that mixed with marine air prior to

774 sampling (Di Lorenzo et al., 2018).

775

776

3.3.3. CHON (O/N ≥ 3) compounds

CHON (O/N ≥ 3) compounds were the dominant compound class in the observed summertime distribution and played an important role in the wintertime distribution as well, comprising 44% of observed functionalized organic aerosol abundance in summer vs. 24% in winter (Figure 3A-B). These contributions were far greater than the contributions of CHON (O/N ≥ 3) species at other sites, which typically ranged from 14-19% (predominantly from summertime measurement, Figure 3C).

Similar to CHON (O/N < 3), we observed some CHON (O/N ≥ 3) compounds with functional groups containing 3 oxygen atoms and 1 nitrogen atom, e.g., nitrophenols and organonitrates (Figure 4), but also contributions from nitrogen-only functional groups paired with oxygen-containing groups. Notably, in the summer, there were important contributions from amines (47% of this compound class's nitrogen content), imines (19%), organonitrates (10%), and azoles (16%) (Figure 4). In contrast, in the winter, nitrogen content in the CHON (O/N ≥ 3) compound class was dominated by I/SVOC nitrophenols, comprising 64% of the CHON (O/N ≥ 3) ion abundance.

NO_x mixing ratios were typically low in both summer and winter (2.3 ± 1.5 ppb in summer vs. 3.7 ± 2.7 ppb in winter), but were slightly higher during winter. In the winter, CHON (O/N ≥ 3) compounds showed a weak positive relationship with NO_x mixing ratios (r ~ 0.58) and a stronger correlation with NO mixing ratios (r ~ 0.81). This relationship between CHON (O/N ≥ 3) and NO (and NO_x) suggests that many of these oxidized nitrogen species were products of NO_x-related chemistry (i.e., NO_z compounds). The enhancements in nitrophenols serves as one example of this, as NO mixing ratios also correlated with the contribution of nitrophenols in the winter (r ~ 0.69).

801   In past work, we discussed nitrophenol nighttime enhancements during winter, and noted

802   their reported aqueous formation pathways mentioned in prior laboratory studies (Ditto et al.,

803   2020). Here, we demonstrate that nitrophenols were important contributors to the CHON (O/N $\geq$

804   3) compound class, and highlight their role as examples of NO_z due to their possible formation

805   via dark aqueous-phase nitration pathways of oxygenated aromatics with ambient nitrous acid

806   (HONO) (Vidović et al., 2018). While nitrophenols may have other sources (e.g., diesel exhaust),

807   our observations of a clear nighttime enhancement during the winter suggest that these functional

808   groups were most likely formed by secondary chemistry related to NO_x oxidation, as this field

809   site was removed from major roadways. Our wintertime observations suggest that HONO could

810   have been derived from local wood burning, and could have reacted away as the smoke plume

811   aged to form stable products like nitrophenols, similar to HONO transformation chemistry into

812   other forms of oxidized nitrogen (e.g., particulate nitrates, PANs, organic nitrates) that has

813   recently been observed in wildfire smoke (Juncosa Calahorrano et al., 2021).

814   Furthermore, the correlation between NO and CHON (O/N $\geq$ 3) could also be influenced

815   by the daytime formation of organonitrates via reaction with $OH^{\bullet}$ and NO (i.e., $RO_2^{\bullet}$ + NO)

816   (Liebmann et al., 2019; Ng et al., 2017; Perring et al., 2013; Takeuchi and Ng, 2018), though

817   organonitrates contributed to a smaller fraction of CHON (O/N $\geq$ 3) species (i.e., 10% of this

818   compound class's nitrogen content across seasons).

819

820   *3.3.4. Overall contributions of reduced and oxidized nitrogen groups*

821   In the summer and winter, contributions from reduced nitrogen groups (e.g., groups

822   shown in black/grey in Figure 4) rivaled that of oxidized nitrogen groups in CHON compounds

823   across a range of O/N ratios. In the summer, reduced nitrogen groups contributed to 50% of all

824   detected CHON (O/N < 3) compounds by ion abundance, while in the winter they contributed

825   47% (Figure 4). For CHON compounds with O/N $\geq$ 3, reduced nitrogen groups contributed to

826   68% of compound ion abundance in the summer (possibly related to marine influences (Wozniak

827   et al., 2014)), while in the winter they contributed just 13%. Interestingly, 90% of the dominant

828   reduced nitrogen functional groups observed (amines and imines) were present in acyclic rather

829   than cyclic structures, which may have been the result of either direct emissions or formation via

830   reactions with ammonia or other small amines.

831   In contrast, possible NO_z products (e.g., groups shown in blue in Figure 4) were present

832   in 18% and 7% of CHON (O/N < 3) compounds in the summer and winter, respectively. For

833   CHON (O/N $\geq$ 3) compounds, they were present in 18% and 86% in the summer and winter,

834   respectively, with the latter wintertime increase in oxidized N-groups largely driven by the

835   presence of nitrophenols at night (Ditto et al., 2020). The remaining fraction of nitrogen-

836   containing groups also contained oxygen, but with a reduced nitrogen atom (e.g., amide,   `Deleted:`

837   isocyanate, nitrogen/oxygen-containing azole, shown in brown in Figure 4). We note that

838   CHONS compounds also represented a sizable fraction of observed organic nitrogen (Figure 3),

839   and contained a mix of reduced and oxidized functional groups (Section S3 and Figures S7-8).   `Deleted: 4`

840   The importance of reduced nitrogen functional groups in CHON compounds highlights

841   that not all oxygen- and nitrogen-containing species in the CHON (O/N $\geq$ 3) compound class

842   were NO_z, despite their apparent molecular formulas and the observed correlation observed

843   between CHON (O/N $\geq$ 3) species with NO and NO_x mixing ratios. For instance, many of the

844   observed reduced nitrogen-containing functional groups co-occurred with several oxygen-

845   containing groups like hydroxyls, carboxylic acids, esters, ethers, and carbonyls, and thus had

848   molecular formulas with O/N ≥ 3, which could incorrectly be assumed to be an organonitrate or

849   similar structure based on molecular formula alone.

850   We note that the relative distribution of reduced and oxidized nitrogen-containing groups

851   shown here is subject to sampling and ionization conditions. While the electrospray ionization

852   source used for the particle-phase analysis discussed here effectively ionized these nitrogen-

853   containing groups, their relative sensitivity may differ because many of these functional groups

854   were present in multifunctional compounds whose other features may also contribute to

855   ionization behavior. Also, other aspects of the sample collection and extraction process could

856   cause variability in observed signal (e.g., PM size cut, organonitrate stability over long duration

857   samples). Thus, we emphasize that the observed relative abundances here are valuable because

858   they suggest that fully reduced nitrogen-containing groups are important contributors to

859   multifunctional CHON species, but their exact mass contributions remain uncertain.

860
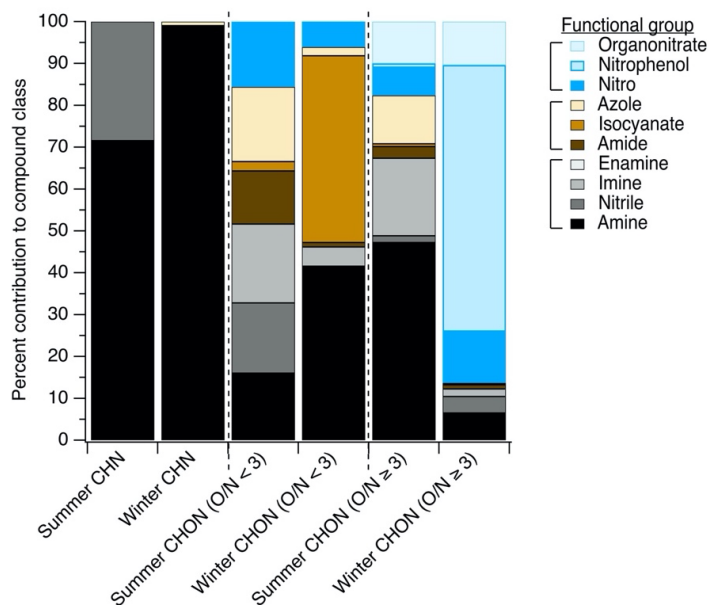
Figure 4. The distribution of functional groups in particle-phase nitrogen-containing compounds measured via LC-ESI-MS/MS. The breakdown of CHN, CHON (O/N < 3), and CHON (O/N ≥ 3) compounds is shown as a function of contributions of each functional group to ion abundance, with possible NO_z species shown in blue shades, fully-reduced nitrogen-containing groups shown in black/grey shades, and groups containing both oxygen and nitrogen where the nitrogen atom itself is not oxidized shown in brown shades. The same data tallied by occurrence are shown in Figure S6 for comparison. Figures S7 and S8 show the functional group distribution for CHNS and CHONS compound classes tallied by abundance and by occurrence, respectively.

3.4. Probing Possible Nitrogen-Containing Gas-Phase Precursors to Observed Nitrogen-Containing Particles with Adsorptive Sampling and LC-ESI-MS

The particle-phase volatility distribution in the winter ranged from IVOC-ULVOC. Of

the observed compounds in winter, 68% contained nitrogen; these likely included contributions

from functionalized gas-phase precursors and likely were influenced by the active multiphase

partitioning of these precursors, and their gas- or particle-phase reaction products, with changes

879   in organic aerosol loading, atmospheric liquid water concentrations, and temperature (Donahue

880   et al., 2011; Ervens et al., 2011). This emphasizes the need to measure a broader range of these

881   functionalized gas-phase compounds, which have known limitations with GC transmission, but

882   represent uncertain and important-to-measure SOA precursors.

883   However, despite evidence of higher volatility particle-phase compounds with diverse

884   nitrogen-containing functionalities that could dynamically partition between phases (Figure 2A-

885   B), the observed compound class distribution from gas-phase adsorbent tube measurements

886   analyzed via GC-APCI-MS was dominated by hydrocarbons (i.e., CH, 24% of detected ion

887   abundance in summer vs. 18% in winter) and oxygenates (i.e., CHO, 66% in summer vs. 69% in

888   winter) (Figure S10-11). These gas-phase species appeared to be lightly functionalized

889   oxygenates (average O/C: 0.12 ± 0.13), showing minimal contributions from nitrogen (or sulfur)

890   heteroatoms; only 9% of detected ion abundance from gas-phase adsorbent tubes in summer and

891   11% in winter contained a nitrogen heteroatom. This is likely due to measurement limitations;

892   while GC-APCI techniques are extremely well-suited for the analysis of less functionalized

893   organic compounds from both instrument transmission and ionization efficiency perspectives,

894   these techniques are not as effective for more polar, more functionalized, more thermally-labile,

895   or otherwise less-GC-amenable species. Thus, to examine a broader range of functionalized gas-

896   phase compounds, we used an offline adsorptive sampling method on cooled PEEK tubing

897   collectors and inline mobile phase desorption for LC-ESI-MS analysis (Figure 1). CH and CHS

898   compound classes were excluded from this gas-phase LC-ESI-MS analysis due to their poor ESI

899   ionization efficiency.

900   Due to variations in trapping and desorption effectiveness (Section S1), this method was

901   not intended to be used as a quantitative measurement of concentration, but rather a relative

| Deleted: | substantial contributions from particle-phase I/SVOCs with |

| Deleted: | S5 |

905   assessment of the distribution of nitrogen-containing gas-phase organic compounds. The

906   variation between analytes in breakthrough testing does not influence our conclusions about the

907   overall prevalence of observed gas-phase organic nitrogen. In laboratory tests, gas-phase sample

908   collection, inline desorption to the mobile phase, trapping on the LC column, and

909   chromatographic separation performed well. We observed limited breakthrough for most

910   analytes during sampling, effective focusing prior to LC analysis, and similar separations for

911   spiked collectors and breakthrough tests compared to standard LC runs (Figure 1B).

912   Results from the application of this new method at the YCFS revealed a wide range of

913   compounds with oxygen-, nitrogen-, and/or sulfur-containing functionality (Figure 5) that existed

914   at a lower average saturation mass concentration than the adsorbent tube methods during winter,

915   with a $\log(C_0)$ of 3.5 ± 3.1 $\mu g/m^3$ for adsorbent tubes analyzed with GC-APCI-MS compared to

916   1.9 ± 2.1 $\mu g/m^3$ for functionalized gases observed via LC-ESI-MS. This decrease in volatility

917   corresponded to an increase in the average O/C ratio of these functionalized gases to 0.24 ± 0.24,

918   which can partly be attributed to LC-ESI's poor ionization of CH compounds and to the

919   collection system's design (targeting heteroatom-containing species and not higher volatility

920   hydrocarbons). This may be a lower limit of O/C among functionalized compounds, as during

921   testing with a mixture of standards, we often observed poor retention of high O/C sugars like

922   xylitol and mannose on the LC analytical column (Table S2).

923   The gas-phase LC-ESI-MS data provide a valuable comparison to the wintertime

924   particle-phase samples analyzed using the same instrument. These particle-phase samples had

925   major contributions from CHO, CHON (O/N < 3 and O/N ≥ 3), CHONS, and CHOS compound

926   classes (Figure 3B). While not collected concurrently, the functionalized gas-phase samples in

927   winter had similar contributions from CHO (20%) and CHON (O/N ≥3) compounds (16%),

928 relatively more CHN (11%) and CHON (O/N < 3) (46%) compounds, and fewer CHONS (2.7%)

929 and CHOS (4.4%) compounds (Figure 5A). The prevalence of gas-phase CHN, CHON (O/N <

930 3), and CHON (O/N ≥ 3) is of particular interest given the abundance of CHON compounds

931 observed in the particle phase, and the potential of these gases to partition to the particle-phase

932 and/or act as reactive precursors to other oxidized nitrogen-containing species.

933   The presence of these nitrogen-containing compounds in the gas-phase also suggests that

934 these compound classes observed in the particle-phase at least partly originated in the gas-phase

935 and partitioned, rather than formed exclusively as a result of particle-phase chemistry. These

936 species could have also formed in the particle-phase and partitioned to the gas-phase with or

937 without condensed-phase fragmentation (discussed above). In either scenario, these nitrogen-

938 containing compounds likely actively partitioned between phases due to their volatility (e.g.,

939 I/SVOCs shown in Figure 5A). Also, their polarity and high Henry's Law coefficients (relative

940 to non-functionalized hydrocarbons (Sander, 2015)) suggests that these compounds could have

941 been readily taken up by the aqueous phase. To check that these compounds were indeed gas-

942 phase species under ambient conditions, we predicted the saturation mass concentration for

943 individual compounds using individual ion formulas and estimated their gas-particle partitioning

944 to a pre-existing condensed phase. While the range of compounds in Figure 5A can be expected

945 to dynamically partition, the results confirm that the overall suite of observed compounds would

946 have predominately existed as gases, with on average ~80% of observed ion abundance predicted

947 to equilibrate to the gas-phase across compound classes (Figure S12-13).

948   Of all the gas-phase species observed with at least one nitrogen atom (i.e., CHN, CHON,

949 CHONS, CHNS), collected in winter, we note that 78% of these compounds had an O/N ratio of

950 less than 3 (Figure 5B), indicating that most of these gas-phase species were not organonitrates,

952 nitrophenols, or other similar structures. This is similar to our particle-phase wintertime results,

953 which showed important contributions from reduced nitrogen-containing groups paired with

954 oxygen-containing groups in CHON (O/N < 3) compounds. Notably, we observed an 11%

955 contribution of gas-phase CHN species with this gas-phase LC-ESI-MS method (Figure 5A), in

956 contrast to 2% CHN in the wintertime particle-phase samples (Figure 3). In the winter particle-

957 phase samples, most CHN compounds contained amines (discussed above), and thus we

958 postulate that these functionalized gas-phase CHN species were possibly also amines that acted

959 as precursors to observed nitrogen-containing particle-phase compounds following oxidation and

960 partitioning (or vice versa).

961   The substantial contribution from CHON with O/N < 3 (46%) to the functionalized gas-

962 phase samples could be linked to less photochemical processing of CHON compounds relative to

963 the particle phase and/or the emissions/oxidation of CHN or CHON compounds. Moreover, in

964 the particle-phase, we observed a weak negative relationship between CHN contribution and

965 hydroxyl group prevalence in summertime measurements (r~ -0.57), which may support the

966 transformation of CHN to CHON compounds via the formation of hydroxyl-containing species.

967 The elemental ratio distribution of these functionalized gases is summarized in Figure S14 and

968 Table S6.
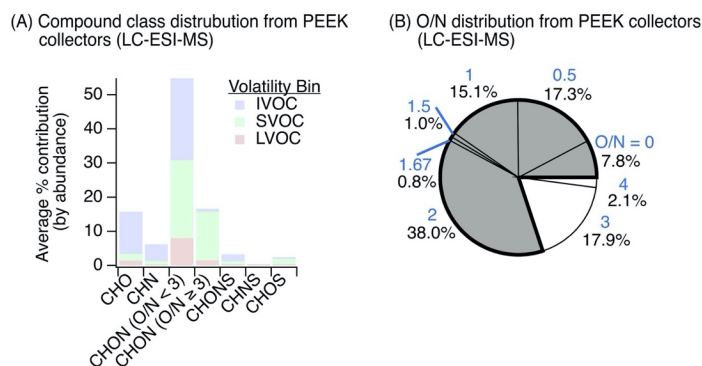
Figure 5. Observations of gas-phase nitrogen-containing compounds. (A) The distribution of functionalized gases observed via sampling on PEEK collectors (N = 6) and inline mobile phase desorption with non-targeted LC-ESI-MS analysis contained a diversity of oxygen-, nitrogen-, and/or sulfur-containing compounds in the IVOC-LVOC range (volatility assignment and grouping was the same as discussed in Figure 2 at a reference temperature of 300 K for intercomparison). While we cannot rule out gas-phase LVOC contributions from evaporation off of the upstream particle filter, LVOC contributions were limited (~12%). (B) Oxygen-to-nitrogen (O/N) ratio distribution of observed gas-phase nitrogen-containing species where O/N ratios < 3 are colored grey and O/N ratios ≥ 3 are colored white (blue text above each percentage signifies the O/N ratio). The same data, tallied by occurrence, are shown in Figure S9 for comparison.

4. Conclusions and Opportunities for Future Research

Together, these results suggest that a mix of direct emissions and chemical processes during summer and winter in the Long Island Sound region resulted in a diverse mixture of multifunctional gases and particles, where more than two-thirds of observed particle-phase compounds contained at least one nitrogen atom.

The observed nitrogen-containing functional groups existed across a range of fully reduced (e.g., amines, imines) to oxidized (e.g., nitro, organonitrate) structures. These fully reduced nitrogen functional groups were prevalent across all nitrogen-containing compound classes, including CHON species, and we highlight their importance as contributors to these multifunctional compounds beyond typical NO_z-type compounds that are commonly studied

992   using online mass spectrometers and share similar CHON molecular formulas. For instance,

993   these gas- and particle-phase measurements of nitrogen-containing compounds are

994   complementary to the measurements of these species made by chemical ionization mass

995   spectrometers (CIMS) or by proton transfer reaction mass spectrometers (PTR-MS), whose

996   ionization mechanisms can be tuned for sensitivity towards functionalized compounds of interest

997   (Riva et al., 2019). While online mass spectrometers excel at high time resolution measurements

998   that capture dynamic chemical processes in the atmosphere, their mass resolution is typically

999   lower and they normally do not utilize separations, so they largely depend on parent ion mass-to-

1000   charge ratios to assign molecular formulas without structural attribution. The offline methods

1001   used here cannot match the time resolution of online techniques. However, the use of

1002   chromatography to separate isomers, longer sampling times to increase sensitivity toward a

1003   greater range of compounds, and the use of higher resolution mass spectrometers with MS/MS

1004   capabilities allow for improved compound identification and determination of functional group

1005   distribution at the molecular level. This enables us to distinguish between true NO_z species and

1006   those that contain combinations of nitrogen and oxygen but are not NO_x oxidation products.

1007   Thus, both these online and offline methods should be employed together to differentiate a wider

1008   range of nitrogen-containing species and to achieve both temporal and chemical resolution.

1009   As discussed throughout this work, the Long Island Sound region is affected by a mixture

1010   of anthropogenic, biogenic, and marine sources, all of which contain known emitters of organic

1011   nitrogen. Understanding the combined effect of these individual sources and their chemical

1012   transformations will be important in regions like the Long Island Sound, where a significant

1013   degree of mixing occurs over the Sound before air parcels arrive inland. For example, past work

1014   has noted extremely high contributions from alkylamines in biomass burning-influenced air

1015 mixed with marine air (Di Lorenzo et al., 2018). Similar enhancements could be expected when

1016 mixing other prominent sources of amines with marine air, such as in the aging urban outflow

1017 from the Central Atlantic and Northeast U.S., which may be transported up the coast and impact

1018 states in the surrounding region.

1019   As with any ambient site, these mixed emissions are chemically processed in the

1020 atmosphere via a multitude of pathways. Here, we observed evidence of photochemical and

1021 aqueous processes occurring in both seasons, but in the winter we observed various mixture-wide

1022 trends that suggested an enhanced role for aqueous-phase processing. These observations

1023 included higher overall particle-phase volatility and smaller carbon backbone sizes, which may

1024 indicate a more important role for aqueous-phase fragmentation reactions or aqueous uptake of

1025 water soluble gases (Brege et al., 2018). We also observed key marker functional groups that

1026 may be formed via aqueous phase chemistry (e.g., nitrophenols, azoles). The role of aqueous-

1027 phase chemistry and aqueous-phase uptake of gases is increasingly studied in laboratory and

1028 ambient contexts (Herrmann et al., 2015), and such chemistry should further examined especially

1029 in coastal and other humid regions.

1030   For example, the aqueous-phase processing of atmospherically relevant nitrogen-

1031 containing species is particularly important to understand in ambient air due to the potential of

1032 brown carbon formation, which has significant impacts on climate forcing (Laskin et al., 2015).

1033 The role of ammonia and amines reacting with carbonyls is of interest for this type of chemistry

1034 (e.g., DeHaan et al., 2009; Grace et al., 2020; McNeill, 2015; Sareen et al., 2010) and should

1035 continue to be explored, particularly in coastal settings where concentrations of small gas-phase

1036 amines may be high due to their marine sources. As discussed above, our ambient observations

1037 of azoles could be indicative of such chemistry, and should be explored in future comparisons of

1038 ambient and laboratory-generated species. Also, we observed a significant contribution from

1039 nitrophenols at our site, and while they are not formed by this same chemistry, they represent

1040 another important form of light absorbing nitrogen-containing organic mass in the atmosphere

1041 (Hems and Abbatt, 2018). Finally, many of the nitrogen-containing functional groups observed

1042 in this work may be susceptible to hydrolysis, so the balance between hydrolysis and other

1043 aqueous pathways is important to consider and understand for appropriate representation of

1044 nitrogen-containing compounds in models for both aqueous aerosol and in-cloud/fog chemistry.

1045   As another example, the greater prevalence overall higher volatility species observed in

1046 the winter particle-phase samples suggested possible dynamic partitioning or aqueous uptake of

1047 lighter gas-phase compounds; to explore the composition of these lighter gas-phase compounds

1048 that could exist as I/SVOCs and thus participate in phase partitioning, we supplemented our

1049 particle-phase analyses with a novel approach for investigating functionalized gases with LC-

1050 ESI-MS. Further investigation of these nitrogen-containing gases will facilitate new

1051 understanding of their gas-particle partitioning in the presence of atmospheric water and organic

1052 condensed species, and measurements across dynamic conditions will help elucidate the relative

1053 importance of both processes. For these types of measurements, further design iterations of the

1054 PEEK sampling system for functionalized gases and additional functionalized gas-phase samples

1055 for LC-ESI-MS analysis could be pursued. Concurrent high volume filter samples could be

1056 collected for direct comparison to the particle-phase, which was not possible in this study due to

1057 insufficient mass loading on the upstream filter during the short duration functionalized gas

1058 sample (i.e., 2 hours). Concurrent PEEK samples could also be collected for MS/MS analysis.

1059   In all, combinations of online and offline mass spectrometry to obtain temporal and

1060 chemical detail, further ambient observations of major organic nitrogen sources, a better

1063 understanding of the aqueous processing of nitrogen-containing compounds, and improved

1064 characterization of their gas-particle partitioning in the presence of atmospheric water will

Deleted: aerosol liquid

1065 together allow for a more accurate representation of nitrogen-containing organic compounds in

1066 emission inventories and models, and enhance our ability to predict their impacts on atmospheric

1067 composition, human health, and climate.

1068

1069 **Author contributions:** J.C.D. and D.R.G. planned the field sampling and study. J.C.D. collected

1070 and analyzed field samples, and performed PEEK sampling and inline LC method development.

1071 J.M. performed inline LC method development. J.C.D. and D.R.G. wrote the manuscript with

1072 contributions from all co-authors.

1073

1074 **Data availability:** Available upon request to Drew R. Gentner (drew.gentner@yale.edu).

Deleted: Data are

Deleted: a

1075

1076 **Competing interests:** The authors declare that they have no substantive conflicts of interest but

1077 acknowledge that D.R.G. is an associate editor with *Atmospheric Chemistry and Physics*.

1078

1079 **Acknowledgements:** We acknowledge support from the National Science Foundation

1080 (AGS1764126) and the Yale Natural Lands Program. J.M. thanks the Goodyear Tire & Rubber

1081 Company and the Grumman Fellowship. We also acknowledge GERSTEL for their collaboration

1082 with the thermal desorption unit used here. We thank David Wheeler at the New York

1083 Department of Environmental Conservation, Pete Babich and Adam Augustine at the

1084 Connecticut Department of Energy and Environmental Protection, Luke Valin at the

1085 Environmental Protection Agency, and Jordan Peccia at Yale for use of sampling equipment, as

1086 well as Paul Miller (NESCAUM) for organizing the LISTOS project. We also thank Richard

Boardman and the Yale Peabody Museum for enabling us to set up and collect samples at the

YCFS site, and acknowledge the help of Yale Peabody Museum EVOLUTIONS interns: Amir

Bond, Ethan Weed, Paula Mock, and Aurea Orencia. We thank Trevor VandenBoer and Barbara

Ervens for helpful feedback on the draft manuscript. Finally, we acknowledge the NOAA Air

Resources Laboratory (ARL) for the provision of the HYSPLIT transport and dispersion model.

References

Altieri, K. E., Turpin, B. J. and Seitzinger, S. P.: Composition of dissolved organic nitrogen in continental precipitation investigated by ultra-high resolution FT-ICR mass spectrometry, Environ. Sci. Technol., 43(18), 6950–6955, doi:10.1021/es9007849, 2009.

Boone, E. J., Laskin, A., Laskin, J., Wirth, C., Shepson, P. B., Stirm, B. H. and Pratt, K. a.: Aqueous Processing of Atmospheric Organic Particles in Cloud Water Collected via Aircraft Sampling, Environ. Sci. Technol., 150611113115005, doi:10.1021/acs.est.5b01639, 2015.

Borduas, N., Da Silva, G., Murphy, J. G. and Abbatt, J. P. D.: Experimental and theoretical understanding of the gas phase oxidation of atmospheric amides with OH radicals: Kinetics, products, and mechanisms, J. Phys. Chem. A, 119(19), 4298–4308, doi:10.1021/jp503759f, 2015.

Brean, J., Dall'Osto, M., Simó, R., Shi, Z., Beddows, D. C. S. and Harrison, R. M.: Open ocean and coastal new particle formation from sulfuric acid and amines around the Antarctic Peninsula, Nat. Geosci., 14(6), 383–388, doi:10.1038/s41561-021-00751-y, 2021.

Brege, M., Paglione, M., Gilardoni, S., Decesari, S., Facchini, M. C. and Mazzoleni, L. R.: Molecular insights on aging and aqueous-phase processing from ambient biomass burning emissions-influenced Po Valley fog and aerosol, Atmos. Chem. Phys., 18(17), 13197–13214, doi:10.5194/acp-18-13197-2018, 2018.

Chen, C. L., Chen, S., Russell, L. M., Liu, J., Price, D. J., Betha, R., Sanchez, K. J., Lee, A. K. Y., Williams, L., Collier, S. C., Zhang, Q., Kumar, A., Kleeman, M. J., Zhang, X. and Cappa, C. D.: Organic Aerosol Particle Chemical Properties Associated With Residential Burning and Fog in Wintertime San Joaquin Valley (Fresno) and With Vehicle and Firework Emissions in Summertime South Coast Air Basin (Fontana), J. Geophys. Res. Atmos., 123(18), 10707–10731, doi:10.1029/2018JD028374, 2018.

Cleveland, W. S., Kleiner, B., McRae, J. E. and Warner, J. L.: Photochemical air pollution: Transport from the New York City area into Connecticut and Massachusetts, Science., 191(4223), 179–181, doi:10.1126/science.1246603, 1976.

Dall'Osto, M., Airs, R. L., Beale, R., Cree, C., Fitzsimons, M. F., Beddows, D., Harrison, R. M., Ceburnis, D., O'Dowd, C., Rinaldi, M., Paglione, M., Nenes, A., Decesari, S. and Simó, R.: Simultaneous Detection of Alkylamines in the Surface Ocean and Atmosphere of the Antarctic Sympagic Environment, ACS Earth Sp. Chem., 3(5), 854–862, doi:10.1021/acsearthspacechem.9b00028, 2019.

Decesari, S., Paglione, M., Rinaldi, M., Dall'osto, M., Simó, R., Zanca, N., Volpi, F., Cristina Facchini, M., Hoffmann, T., Götz, S., Johannes Kampf, C., O'Dowd, C., Ceburnis, D., Ovadnevaite, J. and Tagliavini, E.: Shipborne measurements of Antarctic submicron organic aerosols: An NMR perspective linking multiple sources and bioregions, Atmos. Chem. Phys., 20(7), 4193–4207, doi:10.5194/acp-20-4193-2020, 2020.

DeHaan, D. O., Corrigan, A. L., Smith, K. W., Stroik, D. R., Turley, J. J., Lee, F. E., Tolbert, M. A., Jimenez, J. L., Cordova, K. E., Ferrell, G. R., Haan, D. O. De, Corrigan, A. L., Smith, K. W., Stroik, D. R., Turley, J. J., Lee, F. E.,

Tolbert, M. A., Jimenez, J. L., Cordova, K. E. and Ferrell, G. R.: Secondary organic aerosol-forming reactions of glyoxal with amino acids, Environ. Sci. Technol., 43(8), 2818–2824, doi:10.1021/es803534f, 2009.

Di, Q., Wang, Y., Zanobetti, A., Wang, Y., Koutrakis, P., Choirat, C., Dominici, F. and Schwartz, J. D.: Air pollution and mortality in the medicare population, N. Engl. J. Med., 376(26), 2513–2522, doi:10.1056/NEJMoa1702747, 2017.

Ditto, J. C., Barnes, E. B., Khare, P., Takeuchi, M., Joo, T., Bui, A. A. T., Lee-Taylor, J., Eris, G., Chen, Y., Aumont, B., Jimenez, J. L., Ng, N. L., Griffin, R. J. and Gentner, D. R.: An omnipresent diversity and variability in the chemical composition of atmospheric functionalized organic aerosol, Commun. Chem., 1(1), 75, doi:10.1038/s42004-018-0074-3, 2018.

Ditto, J. C., Joo, T., Khare, P., Sheu, R., Takeuchi, M., Chen, Y., Xu, W., Bui, A. A. T., Sun, Y., Ng, N. L. and Gentner, D. R.: Effects of Molecular-Level Compositional Variability in Organic Aerosol on Phase State and Thermodynamic Mixing Behavior, Environ. Sci. Technol., 53(22), 13009–13018, doi:10.1021/acs.est.9b02664, 2019.

Ditto, J. C., Joo, T., Slade, J. H., Shepson, P. B., Ng, N. L. and Gentner, D. R.: Nontargeted Tandem Mass Spectrometry Analysis Reveals Diversity and Variability in Aerosol Functional Groups across Multiple Sites, Seasons, and Times of Day, Environ. Sci. Technol. Lett., 7(2), 60–69, doi:10.1021/acs.estlett.9b00702, 2020.

Ditto, J. C., He, M., Hass-Mitchell, T. N., Moussa, S. G., Hayden, K., Li, S.-M., Liggio, J., Leithead, A., Lee, P., Wheeler, M. J., Wentzell, J. J. B. and Gentner, D. R.: Atmospheric Evolution of Emissions from a Boreal Forest Fire: The Formation of Highly-Functionalized Oxygen-, Nitrogen-, and Sulfur-Containing Compounds, Atmos. Chem. Phys., 21, 255–267, 2021.

Donahue, N. M., Epstein, S. A., Pandis, S. N. and Robinson, A. L.: A two-dimensional volatility basis set: 1. organic-aerosol mixing thermodynamics, Atmos. Chem. Phys., 11(7), 3303–3318, doi:10.5194/acp-11-3303-2011, 2011.

Dührkop, K., Shen, H., Meusel, M., Rousu, J. and Böcker, S.: Searching molecular structure databases with tandem mass spectra using CSI:FingerID, Proc. Natl. Acad. Sci., 112(41), 12580–12585, doi:10.1073/pnas.1509788112, 2015.

Dührkop, K., Fleischauer, M., Ludwig, M., Aksenov, A. A., Melnik, A. V., Meusel, M., Dorrestein, P. C., Rousu, J. and Böcker, S.: SIRIUS 4: a rapid tool for turning tandem mass spectra into metabolite structure information, Nat. Methods, 16(4), 299–302, doi:10.1038/s41592-019-0344-8, 2019.

Dunlea, E. J., Herndon, S. C., Nelson, D. D., Volkamer, R. M., San Martini, F., Sheehy, P. M., Zahniser, M. S., Shorter, J. H., Wormhoudt, J. C., Lamb, B. K., Allwine, E. J., Gaffney, J. S., Marley, N. A., Grutter, M., Marquez, C., Blanco, S., Cardenas, B., Retama, A., Ramos Villegas, C. R., Kolb, C. E., Molina, L. T. and Molina, M. J.: Evaluation of nitrogen dioxide chemiluminescence monitors in a polluted urban environment, Atmos. Chem. Phys., 7(10), 2691–2704, doi:10.5194/acp-7-2691-2007, 2007.

Ervens, B., Turpin, B. J. and Weber, R. J.: Secondary organic aerosol formation in cloud droplets and aqueous particles (aqSOA): A review of laboratory, field and model studies, Atmos. Chem. Phys., 11(21), 11069–11102, doi:10.5194/acp-11-11069-2011, 2011.

Gaston, C. J., Quinn, P. K., Bates, T. S., Gilman, J. B., Bon, D. M., Kuster, W. C. and Prather, K. A.: The impact of shipping, agricultural, and urban emissions on single particle chemistry observed aboard the R/V Atlantis during CalNex, J. Geophys. Res. Atmos., 118(10), 5003–5017, doi:10.1002/jgrd.50427, 2013.

Ge, X., Wexler, A. S. and Clegg, S. L.: Atmospheric amines - Part I. A review, Atmos. Environ., 45(3), 524–546, doi:10.1016/j.atmosenv.2010.10.012, 2011.

Ge, Y., Liu, Y., Chu, B., He, H., Chen, T., Wang, S., Wei, W. and Cheng, S.: Ozonolysis of Trimethylamine Exchanged with Typical Ammonium Salts in the Particle Phase, Environ. Sci. Technol., 50(20), 11076–11084,

1194   doi:10.1021/acs.est.6b04375, 2016.

1195

1196   Gioda, A., Reyes-Rodríguez, G. J., Santos-Figueroa, G., Collett, J. L., Decesari, S., Ramos, M. D. C. K. V., Bezerra
1197   Netto, H. J. C., De Aquino Neto, F. R. and Mayol-Bracero, O. L.: Speciation of water-soluble inorganic, organic,
1198   and total nitrogen in a background marine environment: Cloud water, rainwater, and aerosol particles, J. Geophys.
1199   Res. Atmos., 116(5), doi:10.1029/2010JD015010, 2011.

1200

1201   de Gouw, J. A., Middlebrook, A. M., Warneke, C., Goldan, P. D., Kuster, W. C., Roberts, J. M., Fehsenfeld, F. C.,
1202   Worsnop, D. R., Canagaratna, M. R., Pszenny, A. A. P., Keene, W. C., Marchewka, M., Bertman, S. B. and Bates,
1203   T. S.: Budget of organic carbon in a polluted atmosphere: Results from the New England Air Quality Study in 2002,
1204   J. Geophys. Res. D Atmos., 110(16), 1–22, doi:10.1029/2004JD005623, 2005.

1205

1206   Grace, D. N., Sharp, J. R., Holappa, R. E., Lugos, E. N., Sebold, M. B., Griffith, D. R., Hendrickson, H. P. and
1207   Galloway, M. M.: Heterocyclic Product Formation in Aqueous Brown Carbon Systems, ACS Earth Sp. Chem.,
1208   3(11), 2472–2481, doi:10.1021/acsearthspacechem.9b00235, 2019.

1209

1210   Grace, D. N., Lugos, E. N., Ma, S., Griffith, D. R., Hendrickson, H. P., Woo, J. L. and Galloway, M. M.: Brown
1211   Carbon Formation Potential of the Biacetyl-Ammonium Sulfate Reaction System, ACS Earth Sp. Chem., 4(7),
1212   1104–1113, doi:10.1021/acsearthspacechem.0c00096, 2020.

1213

1214   Hallquist, M., Wenger, J. C., Baltensperger, U., Rudich, Y., Simpson, D., Claeys, M., Dommen, J., Donahue, N. M.,
1215   George, C., Goldstein, A. H., Hamilton, J. F., Herrmann, H., Hoffmann, T., Iinuma, Y., Jang, M., Jenkin, M. E.,
1216   Jimenez, J. L., Kiendler-Scharr, A., Maenhaut, W., McFiggans, G., Mentel, T. F., Monod, A., Prevot, A. S. H.,
1217   Seinfeld, J. H., Surratt, J. D., Szmigielski, R. and Wildt, J.: The formation, properties and impact of secondary
1218   organic aerosol: current and emerging issues, Atmos. Chem. Phys., 9(14), 5155–5236, doi:10.5194/acp-9-5155-
1219   2009, 2009.

1220

1221   Hems, R. F. and Abbatt, J. P. D.: Aqueous Phase Photo-oxidation of Brown Carbon Nitrophenols: Reaction
1222   Kinetics, Mechanism, and Evolution of Light Absorption, ACS Earth Sp. Chem., 2(3), 225–234,
1223   doi:10.1021/acsearthspacechem.7b00123, 2018.

1224

1225   Herrmann, H., Schaefer, T., Tilgner, A., Styler, S. A., Weller, C., Teich, M. and Otto, T.: Tropospheric Aqueous-
1226   Phase Chemistry: Kinetics, Mechanisms, and Its Coupling to a Changing Gas Phase, Chem. Rev., 115(10), 4259–
1227   4334, doi:10.1021/cr500447k, 2015.

1228

1229   Jerrett, M., Burnett, R. T., Pope, C. A., Ito, K., Thurston, G., Krewski, D., Shi, Y., Calle, E. and Thun, M.: Long-
1230   term ozone exposure and mortality, N. Engl. J. Med., 360(11), 1085–1095, doi:10.1056/NEJMoa0803894, 2009.

1231

1232   Juncosa Calahorrano, J. F., Lindaas, J., O'Dell, K., Palm, B. B., Peng, Q., Flocke, F., Pollack, I. B., Garofalo, L. A.,
1233   Farmer, D. K., Pierce, J. R., Collett, J. L., Weinheimer, A., Campos, T., Hornbrook, R. S., Hall, S. R., Ullmann, K.,
1234   Pothier, M. A., Apel, E. C., Permar, W., Hu, L., Hills, A. J., Montzka, D., Tyndall, G., Thornton, J. A. and Fischer,
1235   E. V.: Daytime Oxidized Reactive Nitrogen Partitioning in Western U.S. Wildfire Smoke Plumes, J. Geophys. Res.
1236   Atmos., 126(4), 1–22, doi:10.1029/2020JD033484, 2021.

1237

1238   Khare, P. and Gentner, D. R.: Considering the future of anthropogenic gas-phase organic compound emissions and
1239   the increasing influence of non-combustion sources on urban air quality, Atmos. Chem. Phys., 18(8), 5391–5413,
1240   doi:10.5194/acp-18-5391-2018, 2018.

1241

1242   Khare, P., Marcotte, A., Sheu, R., Walsh, A. N., Ditto, J. C. and Gentner, D. R.: Advances in offline approaches for
1243   trace measurements of complex organic compound mixtures via soft ionization and high-resolution tandem mass
1244   spectrometry, J. Chromatogr. A, 1598, 163–174, doi:10.1016/j.chroma.2019.03.037, 2019.

1245

1246   Kieloaho, A. J., Hellén, H., Hakola, H., Manninen, H. E., Nieminen, T., Kulmala, M. and Pihlatie, M.: Gas-phase
1247   alkylamines in a boreal Scots pine forest air, Atmos. Environ., 80, 369–377, doi:10.1016/j.atmosenv.2013.08.019,
1248   2013.

1249

Kilian, J. and Kitazawa, M.: The emerging risk of exposure to air pollution on cognitive decline and Alzheimer's disease – Evidence from epidemiological and animal studies, Biomed. J., 41(3), 141–162, doi:10.1016/j.bj.2018.06.001, 2018.

Kim, H., Collier, S., Ge, X., Xu, J., Sun, Y., Jiang, W., Wang, Y., Herckes, P. and Zhang, Q.: Chemical processing of water-soluble species and formation of secondary organic aerosol in fogs, Atmos. Environ., 200(August 2018), 158–166, doi:10.1016/j.atmosenv.2018.11.062, 2019.

Kind, T. and Fiehn, O.: Seven Golden Rules for heuristic filtering of molecular formulas obtained by accurate mass spectrometry., BMC Bioinformatics, 8(1), 105, doi:10.1186/1471-2105-8-105, 2007.

Laskin, A., Laskin, J. and Nizkorodov, S. A.: Chemistry of Atmospheric Brown Carbon, Chem. Rev., 115(10), 4335–4382, doi:10.1021/cr5006167, 2015.

LeClair, J. P., Collett, J. L. and Mazzoleni, L. R.: Fragmentation analysis of water-soluble atmospheric organic matter using ultrahigh-resolution FT-ICR mass spectrometry, Environ. Sci. Technol., 46(8), 4312–4322, doi:10.1021/es203509b, 2012.

Leslie, M. D., Ridoli, M., Murphy, J. G. and Borduas-Dedekind, N.: Isocyanic acid (HNCO) and its fate in the atmosphere: A review, Environ. Sci. Process. Impacts, 21(5), 793–808, doi:10.1039/c9em00003h, 2019.

Li, Y., Pöschl, U. and Shiraiwa, M.: Molecular corridors and parameterizations of volatility in the chemical evolution of organic aerosols, Atmos. Chem. Phys., 16(5), 3327–3344, doi:10.5194/acp-16-3327-2016, 2016.

Liebmann, J., Sobanski, N., Schuladen, J., Karu, E., Hellén, H., Hakola, H., Zha, Q., Ehn, M., Riva, M., Heikkinen, L., Williams, J., Fischer, H., Lelieveld, J. and Crowley, J. N.: Alkyl nitrates in the boreal forest: formation via the NO3-, OH- and O3-induced oxidation of biogenic volatile organic compounds and ambient lifetimes, Atmos. Chem. Phys., 19, 10391–10403, doi:10.5194/acp-2019-463, 2019.

Lim, S., McArdell, C. S. and von Gunten, U.: Reactions of aliphatic amines with ozone: Kinetics and mechanisms, Water Res., 157, 514–528, doi:10.1016/j.watres.2019.03.089, 2019.

Lim, Y. Bin, Kim, H., Kim, J. Y. and Turpin, B. J.: Photochemical organonitrate formation in wet aerosols, Atmos. Chem. Phys., 16(19), 12631–12647, doi:10.5194/acp-16-12631-2016, 2016.

Lin, M., Walker, J., Geron, C. and Khlystov, A.: Organic nitrogen in PM2.5 aerosol at a forest site in the Southeast US, Atmos. Chem. Phys., 10(5), 2145–2157, doi:10.5194/acp-10-2145-2010, 2010.

Lin, P., Laskin, J., Nizkorodov, S. A. and Laskin, A.: Revealing Brown Carbon Chromophores Produced in Reactions of Methylglyoxal with Ammonium Sulfate, Environ. Sci. Technol., 49(24), 14257–14266, doi:10.1021/acs.est.5b03608, 2015.

Di Lorenzo, R. A., Place, B. K., VandenBoer, T. C. and Young, C. J.: Composition of Size-Resolved Aged Boreal Fire Aerosols: Brown Carbon, Biomass Burning Tracers, and Reduced Nitrogen, ACS Earth Sp. Chem., 2(3), 278–285, doi:10.1021/acsearthspacechem.7b00137, 2018.

Loza, C. L., Craven, J. S., Yee, L. D., Coggon, M. M., Schwantes, R. H., Shiraiwa, M., Zhang, X., Schilling, K. A., Ng, N. L., Canagaratna, M. R., Ziemann, P. J., Flagan, R. C. and Seinfeld, J. H.: Secondary organic aerosol yields of 12-carbon alkanes, Atmos. Chem. Phys., 14(3), 1423–1439, doi:10.5194/acp-14-1423-2014, 2014.

Mace, K. A., Kubilay, N. and Duce, R. A.: Organic nitrogen in rain and aerosol in the eastern Mediterranean atmosphere: An association with atmospheric dust, J. Geophys. Res. Atmos., 108(10), doi:10.1029/2002jd002997, 2003a.

Mace, K. A., Artaxo, P. and Duce, R. A.: Water-soluble organic nitrogen in Amazon Basin aerosols during the dry (biomass burning) and wet seasons, J. Geophys. Res. Atmos., 108(16), doi:10.1029/2003jd003557, 2003b.

1306
1307 McNeill, V. F.: Aqueous organic chemistry in the atmosphere: Sources and chemical processing of organic aerosols,
1308 Environ. Sci. Technol., 49(3), 1237–1244, doi:10.1021/es5043707, 2015.
1309
1310 Montero-Martínez, G., Rinaldi, M., Gilardoni, S., Giulianelli, L., Paglione, M., Decesari, S., Fuzzi, S. and Facchini,
1311 M. C.: On the water-soluble organic nitrogen concentration and mass size distribution during the fog season in the
1312 Po Valley, Italy, Sci. Total Environ., 485–486(1), 103–109, doi:10.1016/j.scitotenv.2014.03.060, 2014.
1313
1314 Ng, N. L., Brown, S. S., Archibald, A. T., Atlas, E., Cohen, R. C., Crowley, J. N., Day, D. A., Donahue, N. M., Fry,
1315 J. L., Fuchs, H., Griffin, R. J., Guzman, M. I., Herrmann, H., Hodzic, A., Iinuma, Y., Kiendler-Scharr, A., Lee, B.
1316 H., Luecken, D. J., Mao, J., McLaren, R., Mutzel, A., Osthoff, H. D., Ouyang, B., Picquet-Varrault, B., Platt, U.,
1317 Pye, H. O. T., Rudich, Y., Schwantes, R. H., Shiraiwa, M., Stutz, J., Thornton, J. A., Tilgner, A., Williams, B. J. and
1318 Zaveri, R. A.: Nitrate radicals and biogenic volatile organic compounds: oxidation, mechanisms, and organic
1319 aerosol, Atmos. Chem. Phys., 17(3), 2103–2162, doi:10.5194/acp-17-2103-2017, 2017.
1320
1321 Perring, A. E., Pusede, S. E. and Cohen, R. C.: An Observational Perspective on the Atmospheric Impacts of Alkyl
1322 and Multifunctional Nitrates on Ozone and Secondary Organic Aerosol, Chem. Rev., 113(8), 5848–5870,
1323 doi:10.1021/cr300520x, 2013.
1324
1325 van Pinxteren, M., Müller, C., Iinuma, Y., Stolle, C. and Herrmann, H.: Chemical Characterization of Dissolved
1326 Organic Compounds from Coastal Sea Surface Microlayers (Baltic Sea, Germany), Environ. Sci. Technol., 46(19),
1327 10455–10462, doi:10.1021/es204492b, 2012.
1328
1329 van Pinxteren, M., Fomba, K. W., van Pinxteren, D., Triesch, N., Hoffmann, E. H., Cree, C. H. L., Fitzsimons, M.
1330 F., von Tümpling, W. and Herrmann, H.: Aliphatic amines at the Cape Verde Atmospheric Observatory:
1331 Abundance, origins and sea-air fluxes, Atmos. Environ., 203, 183–195, doi:10.1016/j.atmosenv.2019.02.011, 2019.
1332
1333 Pope, C. A. and Dockery, D. D.: Health Effects of Fine Particulate Air Pollution: Lines that Connect, J. Air Waste
1334 Manage. Assoc., 56, 709–742, doi:10.1080/10473289.2006.10464485, 2006.
1335
1336 Priestley, M., Le Breton, M., Bannan, T. J., Leather, K. E., Bacak, A., Reyes-Villegas, E., De Vocht, F., Shallcross,
1337 B. M. A., Brazier, T., Khan, M. A., Allan, J., Shallcross, D. E., Coe, H. and Percival, C. J.: Observations of
1338 Isocyanate, Amide, Nitrate, and Nitro Compounds From an Anthropogenic Biomass Burning Event Using a ToF-
1339 CIMS, J. Geophys. Res. Atmos., 123, 7687–7704, doi:10.1002/2017JD027316, 2018.
1340
1341 Pye, H. O. T., Nenes, A., Alexander, B., Ault, A. P., Barth, M. C., Clegg, S. L., Collett, J. L., Fahey, K. M.,
1342 Hennigan, C. J., Herrmann, H., Kanakidou, M., Kelly, J. T., Ku, I. T., Faye McNeill, V., Riemer, N., Schaefer, T.,
1343 Shi, G., Tilgner, A., Walker, J. T., Wang, T., Weber, R., Xing, J., Zaveri, R. A. and Zuend, A.: The acidity of
1344 atmospheric particles and clouds., 2020.
1345
1346 Quinn, P. K., Collins, D. B., Grassian, V. H., Prather, K. A. and Bates, T. S.: Chemistry and Related Properties of
1347 Freshly Emitted Sea Spray Aerosol, Chem. Rev., 115(10), 4383–4399, doi:10.1021/cr500713g, 2015.
1348
1349 Rindelaub, J. D., Borca, C. H., Hostetler, M. A., Slade, J. H., Lipton, M. A., Slipchenko, L. V. and Shepson, P. B.:
1350 The acid-catalyzed hydrolysis of an α-pinene-derived organic nitrate: Kinetics, products, reaction mechanisms, and
1351 atmospheric impact, Atmos. Chem. Phys., 16(23), 15425–15432, doi:10.5194/acp-16-15425-2016, 2016.
1352
1353 Riva, M., Rantala, P., Krechmer, J. E., Peräkylä, O., Zhang, Y., Heikkinen, L., Garmash, O., Yan, C., Kulmala, M.,
1354 Worsnop, D. and Ehn, M.: Evaluating the performance of five different chemical ionization techniques for detecting
1355 gaseous oxygenated organic species, Atmos. Meas. Tech., 12, 2403–2421, doi:https://doi.org/10.5194/amt-12-2403-
1356 2019, 2019.
1357
1358 Roberts, J. M., Veres, P. R., VandenBoer, T. C., Warneke, C., Graus, M., Williams, E. J., Lefer, B., Brock, C. A.,
1359 Bahreini, R., Ozturk, F., Middlebrook, A. M., Wagner, N. L., Dube, W. P. and DeGouw, J. A.: New insights into
1360 atmospheric sources and sinksof isocyanic acid, HNCO, from recent urbanand regional observations, J. Geophys.
1361 Res. Atmos., 119, 1060–1072, doi:10.1002/2013JD019931, 2014.

Rogers, H. M., Ditto, J. C. and Gentner, D. R.: Evidence for impacts on surface-level air quality in the northeastern US from long-distance transport of smoke from North American fires during the Long Island Sound Tropospheric Ozone Study (LISTOS) 2018, Atmos. Chem. Phys., 20(2), 671–682, doi:10.5194/acp-20-671-2020, 2020.

Ruggeri, G. and Takahama, S.: Technical Note: Development of chemoinformatic tools to enumerate functional groups in molecules for organic aerosol characterization, Atmos. Chem. Phys., 16, 4401–4422, doi:10.5194/acp-16-4401-2016, 2016.

Sander, R.: Compilation of Henry's law constants (version 4.0) for water as solvent, Atmos. Chem. Phys., 15(8), 4399–4981, doi:10.5194/acp-15-4399-2015, 2015.

Sareen, N., Schwier, A. N., Shapiro, E. L., Mitroo, D. and Mcneill, V. F.: Secondary organic material formed by methylglyoxal in aqueous aerosol mimics, Atmos. Chem. Phys., 10, 997–1016, doi:10.5194/acpd-9-15567-2009, 2010.

Schervish, M. and Donahue, N. M.: Peroxy radical chemistry and the volatility basis set, Atmos. Chem. Phys., 20(2), 1183–1199, doi:10.5194/acp-20-1183-2020, 2020.

Schroder, J. C., Campuzano-Jost, P., Day, D. A., Shah, V., Larson, K., Sommers, J. M., Sullivan, A. P., Campos, T., Reeves, J. M., Hills, A., Hornbrook, R. S., Blake, N. J., Scheuer, E., Guo, H., Fibiger, D. L., McDuffie, E. E., Hayes, P. L., Weber, R. J., Dibb, J. E., Apel, E. C., Jaeglé, L., Brown, S. S., Thornton, J. A. and Jimenez, J. L.: Sources and Secondary Production of Organic Aerosols in the Northeastern United States during WINTER, J. Geophys. Res. Atmos., 123(14), 7771–7796, doi:10.1029/2018JD028475, 2018.

Schurman, M. I., Boris, A., Desyaterik, Y. and Collett, J. L.: Aqueous secondary organic aerosol formation in ambient cloud water photo-oxidations, Aerosol Air Qual. Res., 18(1), 15–25, doi:10.4209/aaqr.2017.01.0029, 2018.

Sheu, R., Marcotte, A., Khare, P., Charan, S., Ditto, J. C. and Gentner, D. R.: Advances in offline approaches for chemically speciated measurements of trace gas-phase organic compounds via adsorbent tubes in an integrated sampling-to-analysis system, J. Chromatogr. A, 1575, 80–90, doi:10.1016/j.chroma.2018.09.014, 2018.

Sintermann, J. and Neftel, A.: Ideas and perspectives: On the emission of amines from terrestrial vegetation in the context of new atmospheric particle formation, Biogeosciences, 12(11), 3225–3240, doi:10.5194/bg-12-3225-2015, 2015.

Sodeman, D. A., Toner, S. M. and Prather, K. A.: Determination of Single Particle Mass Spectral Signatures from Light-Duty Vehicle Emissions, Environ. Sci. Technol., 39(12), 4569–4580, doi:10.1016/j.atmosenv.2007.01.025, 2005.

Sullivan, A. P., Guo, H., Schroder, J. C., Campuzano-Jost, P., Jimenez, J. L., Campos, T., Shah, V., Jaeglé, L., Lee, B. H., Lopez-Hilfiker, F. D., Thornton, J. A., Brown, S. S. and Weber, R. J.: Biomass Burning Markers and Residential Burning in the WINTER Aircraft Campaign, J. Geophys. Res. Atmos., 124(3), 1846–1861, doi:10.1029/2017JD028153, 2019.

Takeuchi, M. and Ng, N. L.: Organic nitrates and secondary organic aerosol (SOA) formation from oxidation of biogenic volatile organic compounds, ACS Symp. Ser. Multiph. Environ. Chem. Atmos., 1299, 105–125, doi:10.1021/bk-2018-1299.ch006, 2018.

Tao, Y., Liu, T., Yang, X. and Murphy, J. G.: Kinetics and Products of the Aqueous Phase Oxidation of Triethylamine by OH, ACS Earth Sp. Chem., 5(8), 1889–1895, doi:10.1021/acsearthspacechem.1c00162, 2021.

United States Environmental Protection Agency: Historical Exceedance Days in New England, Reg. 1 EPA New Engl. [online] Available from: https://www3.epa.gov/region1/airquality/standard.html (Accessed 14 August 2021), 2020.

VandenBoer, T. C., Petroff, A., Markovic, M. Z. and Murphy, J. G.: Size distribution of alkyl amines in continental particulate matter and their online detection in the gas and particle phase, Atmos. Chem. Phys., 11(9), 4319–4332, doi:10.5194/acp-11-4319-2011, 2011.

Vidović, K., Lašič Jurković, D., Šala, M., Kroflič, A. and Grgić, I.: Nighttime Aqueous-Phase Formation of Nitrocatechols in the Atmospheric Condensed Phase, Environ. Sci. Technol., 52(17), 9722–9730, doi:10.1021/acs.est.8b01161, 2018.

Warneke, C., McKeen, S. A., de Gouw, J. A., Goldan, P. D., Kuster, W. C., Holloway, J. S., Williams, E. J., Lerner, B. M., Parrish, D. D., Trainer, M., Fehsenfeld, F. C., Kato, S., Atlas, E. L., Baker, A. and Blake, D. R.: Determination of urban volatile organic compound emission ratios and comparison with an emissions database, J. Geophys. Res. Atmos., 112(10), 1–13, doi:10.1029/2006JD007930, 2007.

Wozniak, A. S., Willoughby, A. S., Gurganus, S. C. and Hatcher, P. G.: Distinguishing molecular characteristics of aerosol water soluble organic matter from the 2011 trans-North Atlantic US GEOTRACES cruise, Atmos. Chem. Phys., 14(16), 8419–8434, doi:10.5194/acp-14-8419-2014, 2014.

Wu, C., Wen, Y., Hua, L., Jiang, J., Xie, Y., Cao, Y., Chai, S., Hou, K. and Li, H.: Rapid and highly sensitive measurement of trimethylamine in seawater using dynamic purge-release and dopant-assisted atmospheric pressure photoionization mass spectrometry, Anal. Chim. Acta, 1137, 56–63, doi:10.1016/j.aca.2020.08.060, 2020.

Xu, Y., Miyazaki, Y., Tachibana, E., Sato, K., Ramasamy, S., Mochizuki, T., Sadanaga, Y., Nakashima, Y., Sakamoto, Y., Matsuda, K. and Kajii, Y.: Aerosol Liquid Water Promotes the Formation of Water-Soluble Organic Nitrogen in Submicrometer Aerosols in a Suburban Forest, Environ. Sci. Technol., 54(3), 1406–1414, doi:10.1021/acs.est.9b05849, 2020.

Ye, C., Zhou, X., Pu, D., Stutz, J., Festa, J., Spolaor, M., Tsai, C., Cantrell, C., Mauldin, R. L., Campos, T., Weinheimer, A., Hornbrook, R. S., Apel, E. C., Guenther, A., Kaser, L., Yuan, B., Karl, T., Haggerty, J., Hall, S., Ullmann, K., Smith, J. N., Ortega, J. and Knote, C.: Rapid cycling of reactive nitrogen in the marine boundary layer, Nature, 532, 489–491, doi:10.1038/nature17195, 2016.

Youn, J. S., Crosbie, E., Maudlin, L. C., Wang, Z. and Sorooshian, A.: Dimethylamine as a major alkyl amine species in particles and cloud water: Observations in semi-arid and coastal regions, Atmos. Environ., 122, 250–258, doi:10.1016/j.atmosenv.2015.09.061, 2015.

Yu, L., Smith, J., Laskin, A., M George, K., Anastasio, C., Laskin, J., M Dillner, A. and Zhang, Q.: Molecular transformations of phenolic SOA during photochemical aging in the aqueous phase: Competition among oligomerization, functionalization, and fragmentation, Atmos. Chem. Phys., 16(7), 4511–4527, doi:10.5194/acp-16-4511-2016, 2016.

Zhang, J., Ninneman, M., Joseph, E., Schwab, M. J., Shrestha, B. and Schwab, J. J.: Mobile Laboratory Measurements of High Surface Ozone Levels and Spatial Heterogeneity During LISTOS 2018: Evidence for Sea Breeze Influence, J. Geophys. Res. Atmos., 125(11), 1–12, doi:10.1029/2019JD031961, 2020.

Zhang, Q., Anastasio, C. and Jimenez-Cruz, M.: Water-soluble organic nitrogen in atmospheric fine particles (PM2.5) from northern California, J. Geophys. Res. D Atmos., 107(11), 1–9, doi:10.1029/2001jd000870, 2002.

Zhao, Y., Hallar, A. G. and Mazzoleni, L. R.: Atmospheric organic matter in clouds: Exact masses and molecular formula identification using ultrahigh-resolution FT-ICR mass spectrometry, Atmos. Chem. Phys., 13(24), 12343–12362, doi:10.5194/acp-13-12343-2013, 2013.

Zhou, S., Collier, S., Xu, J., Mei, F., Wang, J., Lee, Y.-N., Sedlacek, A. J., Springston, S. R., Sun, Y. and Zhang, Q.: Influences of upwind emission sources and atmospheric processing on aerosol chemistry and properties at a rural location in the Northeastern U.S., J. Geophys. Res. Atmos., 121(10), 6049–6065, doi:10.1002/2015JD024568, 2016.